HHS Public Access

Author manuscript

Food Chem Toxicol. Author manuscript; available in PMC 2020 February 01.

Published in final edited form as:

Food Chem Toxicol. 2019 February ; 124: 112–127. doi:10.1016/j.fct.2018.11.048.

ZnO Nanoparticles Affect Nutrient Transport in an *In Vitro* Model of the Small Intestine

Fabiola Moreno-Olivas[1], **Elad Tako**[2], and **Gretchen J. Mahler**[1,*]

[1]Department of Biomedical Engineering, Binghamton University, Binghamton, NY 13902, USA

[2]Plant, Soil and Nutrition Laboratory, Agricultural Research Services, U.S. Department of Agriculture, Ithaca, NY, 14850, USA

Abstract

Nano-sized zinc oxide (ZnO) is present in food packaging, putting consumers at risk of ingestion. There is little information on the amount of ZnO nanoparticles (NP) present in food packaging and the effects of ZnO NP ingestion on intestinal function. To estimate physiologically relevant ZnO NP exposures from food that are commonly packaged with ZnO NP, food samples were analyzed with inductively coupled plasma mass spectrometry (ICP-MS). An *in vitro* model of the small intestine was used to investigate the effects of ZnO NP exposure. Cells were exposed to pristine NP in culture medium and to NP subjected to an *in vitro* digestion process to better reflect the transformation that the NP undergo in the human gastrointestinal (GI) tract. The findings show that a physiologically relevant dose of ZnO NP can cause a significant decrease in glucose transport, which is consistent with gene expression changes for the basolateral glucose transporter GLUT2. There is also evidence that the ZnO NP affect the microvilli of the intestinal cells, therefore reducing the amount of surface area available to absorb nutrients. These results suggest that the ingestion of ZnO NP can alter nutrient absorption in an *in vitro* model of the human small intestine.

Graphical Abstract

*Corresponding author: Gretchen J. Mahler, PO Box 6000, Binghamton, NY 13902, gmahler@binghamton.edu, (607) 777-5238.

Conflicts of Interest

There are no conflicts of interest to declare.

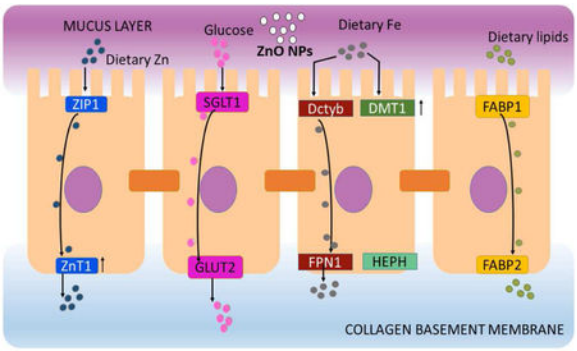

Keywords

Caco-2; HT29-MTX; iron; zinc; glucose; intestinal alkaline phosphatase

1. Introduction

Nanoparticles (NP) have different properties than their bulk counterparts because of their high surface area to volume ratio. While a 90 nm particle has less than 10% of its total atoms on the surface, a 10 nm nanoparticle has more than 40% of its atoms on the surface (Auffan et al., 2009). This makes nanoparticles significantly more reactive. NP have more sites available to donate or receive electrons and therefore can interact with surrounding elements more readily than larger particles. This unique property explains why nanotechnology has become an integral part of society, and currently thousands of consumer products including catalysts, paints, sunscreens, cosmetics, sprays, clothing, and food contain NP (Project on Emerging Nanotechnologies, 2013). The widespread usage of NP in consumer products makes ingestion likely, either unintentionally or via drinking water or the food chain. Despite their wide use, regulations on the amount of nanomaterials that go into consumer products are scarce, and often consumers are unaware that nanomaterials are present in the products they use on a daily basis (Renn and Roco, 2006). While specific food information is becoming more transparent, this is not the case with nanomaterials added into food or packaging that is in direct contact with food. With this in mind, researchers have studied and demonstrated that silicon dioxide (SiO_2), titanium dioxide (TiO_2), and other NP leach into food (Fröhlich and Fröhlich, 2016; Weir et al., 2012).

Zinc oxide (ZnO) NP are used for food packaging due to their antimicrobial properties (Chaudhry et al., 2008; Espitia et al., 2016, 2012) and for decades ZnO has been used in the cans of sulfur-producing foods (Alo, 1965; Hekal and Erlandson, 1981; Kalberg, 1951; Pierce and James, 1969; Rocquet and Auburn, 1970). When the tinplate surface of the cans reacts with sulfur released from meats and certain vegetables, a black tin sulfide stain is formed. To avoid the unsightly stain, ZnO is used so that zinc sulfide is formed instead and the food inside the cans remains appealing for customers (Alo, 1965; Rocquet and Auburn, 1970). Food packaging and manufacturing books, as well as patents, describe the ZnO used in cans as “fine-particle-sized” or “finely divided precipitated ZnO,” but do not have a comprehensive characterization of the ZnO particles or nanoparticles used. Some patents do not state the amount of ZnO contained in cans and others state that the can enamels contain

15% to 40% ZnO (Barret et al., 2005; Robertson, 2012; Yam, 2009). Ultimately, there is no way for consumers to find information about the form of ZnO that is added to the cans of foods they purchase.

There are fewer studies of Zn leaching into food when compared with other types of NP, and therefore scientists use maximum tolerated doses in their studies or arbitrary concentrations that are not based on exposure data (Abbott Chalew and Schwab, 2013; Chia et al., 2015; Chia and Leong, 2016; Heng et al., 2011; Song et al., 2014; Zijno et al., 2015). In these studies, no rationale is given as to why the authors chose to work with these concentrations of NP. Some of the doses used are very high and realistically humans would not consume these amounts of zinc from food. Therefore, we do not know how the consumption of ZnO nanoparticles at physiologically realistic dosages can affect human health. The goal of this study is to investigate the functional effects of a range of ZnO NP doses that included physiologically realistic ZnO NP doses in an *in vitro* model of the gastrointestinal (GI) tract.

Given that absorption of nutrients and redistribution into the bloodstream occurs in the small intestine, this is an ideal organ to model *in vitro* to study the effects of NP ingestion. (Tiede et al., 2008). There is growing evidence that different types of nanoparticles added to food contact materials can affect the small intestine permeability, affect the healthy balance of the gut microbiota, and induce immune responses by directly interacting with immune cells (Groh et al., 2017). In order to model the small intestine, we used one of the most common immortalized cells lines, Caco-2, which is a human colon adenocarcinoma cell line. This cell line has been used extensively for the past 20 years for the development of drugs and for other pharmacological and toxicological studies. This is because the cells can differentiate into absorptive enterocytes that exhibit characteristics such as microvilli, tight junctions, and nutrient transporters (García-Rodríguez et al., 2018; Mahler et al., 2009a, 2009b). The co-culture of Caco-2 cells with another immortalized cell line, HT29-MTX mucus secreting goblet-like cells, has been shown to create a more realistic model because these cells produce a mucus layer that completely covers the monolayer (Kumar et al., 2010; Lesuffleur et al., 1990; Mahler et al., 2012). The inclusion of a mucus layer in NP studies is essential as the mucus layer of the small intestine is the first line of protection for this organ (Hansson, 2012). Previous studies have shown that a mucus layer has a size-dependent effect on NP absorption in the intestinal mucosa (Hillyer and Albrecht, 2001), and that ZnO NP have greater mobility in mucosa and can therefore cause more pulmonary toxicity (Jachak et al., 2012). A more recent study performed in nasal mucosal cells suggests that ZnO NP are capable of inducing pro-inflammatory responses and DNA damage (Hackenberg et al., 2011).

ZnO NP are amphoteric and therefore more prone to dissolution than other NP commonly used in foods, such as TiO_2, and SiO_2 (Tso et al., 2010). The ZnO NP may leach from the can lining into the food, as demonstrated in a study that used propylene containers (Liu et al., 2016). To estimate an *in vitro* dose of ZnO, we purchased cans of naturally low-zinc food from the supermarket and analyzed the food for Zn content. After determining the Zn concentration in commercially available food, we next asked whether this amount of zinc in the form of ZnO NP would have any effect on small intestinal function of a realistic *in vitro* model. We recreated the doses determined from food using ZnO NP and tested the effect of

ZnO NP exposure on the absorption of nutrients in our *in vitro* model of the small intestine. To our knowledge, this is the first study that has tested canned food for Zn content and used these estimated Zn amounts to investigate more physiologically relevant dose exposure of ZnO NP in an *in vitro* model of the small intestine.

2. Materials and Methods

2.1 ZnO dose calculations

Three different brands of canned foods were purchased in the supermarket and the food samples were removed from 3 different areas of the can: the lining, the middle, and the fluid that accumulates at the bottom. These samples were weighed before and after freeze-drying for 72 hours (Labconco Freezone, Marshall Scientific) and then ground into powder. A 100 mg aliquot of the food powder was placed in microcentrifuge tubes in triplicate and then digested with 70% HNO_3. Zn concentration was measured using inductively coupled plasma mass spectrometry (ICP-MS). The resulting amount was converted to NP per serving and then divided by the surface area of the small intestine to determine a standard dose. To represent a range of exposures, a medium dose was determined to be two orders of magnitude higher than the standard (low) dose, and the high dose two orders of magnitude higher than the medium dose, which is comparable to amounts used in similar studies performed with Caco-2 cells (Abbott Chalew and Schwab, 2013; Chia and Leong, 2016; Heng et al., 2011; Song et al., 2014; Zijno et al., 2015). Theses doses are referred to as low, medium and high throughout this article.

2.2 *In vitro* digestion

In order to simulate more realistic conditions of NP ingestion, the 3 concentrations of NP were subjected to a well-established *in vitro* digestion process first described by Glahn et al. (Glahn et al., 1998). This *in vitro* digestion process contains approximate concentrations of salts and enzymes as in the stomach and duodenum. The resulting samples were referred to as “digested NP” and they were warmed in the water bath to 37 °C before being added to the cell cultures. The detailed *in vitro* digestion process can be found in the supplementary information (SI).

2.3 Nanoparticle characterization

The size distributions and average ζ- potentials of 10 nm ZnO NP (Meliorum Technologies, Inc., Rochester, NY) at a concentration of 0.1 mg/mL in 18 MΩ deionized (DI) water were measured with a Zetasizer Nano ZS (Malvern Instruments Inc., Southborough, MA) and the size of the nanoparticles was confirmed using nanoparticle tracking analysis (NTA) with a Malvern Nanosight. A drop of a suspension containing 0.1 mg/mL of ZnO NP in methanol was added to a 400 mesh copper transmission electron microscopy (TEM) grid (Ted Pella, Inc.) with a plastic transfer pipette and allowed to dry overnight. The same grids were used for transmission and scanning electron microscopy (SEM) techniques (TEM, JEOL JEM-2100F and LEO Zeiss Field Emission SEM). For the characterization of ZnO NP in complex biological media such as Dulbecco’s Modified Eagle Medium (DMEM) containing 10% heat-inactivated fetal bovine serum (HI-FBS) and digest, TEM was used. These complex suspensions were prepared immediately before measurement by diluting a 1mg/mL

ZnO NP suspension to the desired concentrations: 9.7×10^{-6} mg/mL, 9.7×10^{-4} mg/mL and 9.7×10^{-2} mg/mL for the low, medium and high concentrations, respectively. Nanoparticles diluted in DMEM were sonicated for 30 minutes (VWR® Symphony™ Ultrasonic Cleaners, RF-48 W, 35k Hz operation frequency), and NP diluted in digests were not sonicated but warmed and used immediately after the previously described digestion procedure. A drop of solution was added to an ultrathin 400 mesh copper TEM grid with a plastic transfer pipette. The grids were allowed to air-dry overnight before TEM imaging.

2.4 Cell culture

The Caco-2 cell line was obtained from the American Type Culture Collection (Manassas, VA, USA) at Passage 17 and used in experiments at Passage 30-45. The HT29-MTX cell line was provided by Dr. Thecla Lesuffleur of INSERM U560 in Lille, France, at Passage 11 and used in experiments at Passage 18-33 (Lesuffleur et al., 1990). The cells were seeded onto 8 μg/cm^2 collagen I coated well plates (Corning Life Sciences, Corning, NY) or Transwells (Corning).

Cells were seeded at a ratio of 3:1 Caco-2 to HT29-MTX, respectively (Mahler et al., 2009b). This ratio represents the ratio of enterocytes to goblet cells required to form the characteristic mucus layer from the intestinal epithelium (Mahler et al., 2009b). Transwell inserts (0.4 μm pore size, 0.33 cm^2) or 24 well plates (Corning) were coated with 8μg/cm^2 rat tail type I collagen (BD Biosceinces, San Jose, CA) and cell monolayers were seeded at a density of 100,000 cells/cm^2 (Transwells) or 50,000 cells/cm^2 (well plates). The monolayers were maintained in high glucose Dulbecco's Modified Eagle Medium (DMEM, Thermo Fisher Scientific, Waltham, MA USA) with 10% (v/v) heat inactivated fetal bovine serum (HI-FBS, Thermo Fisher Scientific), which was changed every other day. All experiments were performed after a cell growth period of 2 weeks. Monolayers were exposed to ZnO NP suspended in DMEM or in the previously described *in vitro* digestion solution for 4 hours before additional assays were performed, these are referred to as “undigested NP” and “digested NP” respectively throughout this article. More detailed information can be found in the SI.

2.5 Nanoparticle Exposure

For NP exposure in Transwell inserts, 100 μL of the undigested or digested NP solutions were added to the apical chamber, while DMEM was added to the basolateral chamber. In the case of the 24 and 96 well plates, undigested ZnO NP suspended in DMEM were added directly to each well and in the case of digests, the ZnO concentrations were doubled to perform the digestions and then diluted at a 1:1 ratio in DMEM with 10% HI-FBS to result in the desired concentration of digested ZnO NP. This was to ensure that the cells were exposed to digested nanoparticles but also received the nutrients necessary from culture medium. Cells were incubated with NP at 37 °C and 5% CO_2 on a rocking shaker (Laboratory Instrument Model RP-50, Rockville, MD) at 6 oscillations per minute for 4 hours.

2.6 Cell viability

Cell viability following digested or undigested NP exposure was assessed with Calcein AM/ Propidium Iodide for live/dead staining (Thermo Fisher Scientific) following the protocol described by the manufacturer (Invitrogen Molecular Probes, 2005). In addition, the cells were imaged with a fluorescent microscope using a 10X objective (Nikon Eclipse Ti, Boston Industries) to confirm the viability results. Detailed information can be found in the SI.

2.7 Transepithelial electrical resistance

Transepithelial electrical resistance (TEER) of the monolayers was measured before and after a 4 hour exposure to the control, low, medium and high digested and undigested nanoparticle concentrations with the EVOM2 and Endohm-6 chamber (World Precision Instruments, Sarasota, FL). More information can be found in the SI.

2.8 Immunocytochemistry

Standard immunocytochemistry techniques were used to stain for the tight junction protein occludin. The cells were fixed with 4% paraformaldehyde (PFA) in phosphate buffered saline (PBS) at room temperature for 50 minutes. Cells were then incubated with 0.1% Triton-X100 in PBS for 5 minutes to permeabilize, washed with PBS, and incubated with PBS containing 5% bovine serum albumin (BSA, Rockland Immunochemicals, Inc., Gilbertsville, PA) on a rotating shaker for 1 hour. A mouse *anti*-occludin primary antibody (Thermo Fisher Scientific) was added to the cells at a 1:100 dilution in PBS and incubated for 2 hours, samples were then rinsed with PBS, and then Alexa Fluor 568 goat *anti*-mouse secondary antibody (1:200 dilution in PBS, Thermo Fisher Scientific) was added to each membrane and incubated for another 2 hours at room temperature in the dark. After a final rinse with PBS, DNA was stained with DRAQ5 (1:1000 in PBS, Thermo Fisher Scientific) for 30 minutes in the dark. After rinsing the cells with 18 MΩ DI water, the membranes were carefully cut using a razor blade and mounted on glass slides with ProLong Gold mounting medium (Thermo Fisher Scientific). The samples were viewed with a Leica TCS SP5 confocal microscope.

2.9 ^{58}Fe and ^{67}Zn transport

ZnO NP exposure and mineral (Fe and Zn) uptake and transport experiments were performed in serum free, very low zinc and iron (<8 μg/L) minimum essential media (MEM). Detailed formulation of this media can be found in Guo et al. (Guo et al., 2017). Cells were washed with PBS and cultured in low-mineral MEM 1 day before the NP and mineral transport experiments to deplete the cells of Zn and Fe. Iron or zinc experimental medium was prepared using ^{58}Fe or ^{67}Zn stable isotopes (Isoflex, San Francisco, CA). 100 μL of the mineral transport medium was added to the apical chamber immediately after nanoparticle exposure. After adding the mineral transport medium, cells were incubated at 37 °C and 5% CO_2 for 2 hours. The cell medium from the basolateral chamber was collected into a sterile 1.5 mL centrifuge tube and 10 μl of ultrapure HNO_3 (Sigma Aldrich, ≥99.999% trace metals basis) was added. Samples were stored at 4 °C until ^{58}Fe and ^{67}Zn and then quantified with ICP-MS. Detailed information on ICP-MS methods was previously described by Guo et al. (Guo et al., 2017).

2.10 Glucose Transport

Cells were starved for 1 hour before glucose transport experiments in serum-free, glucose-free, phenol red-free DMEM (Thermo Fisher Scientific). Glucose transport across monolayers on Transwell permeable supports was measured using the fluorescent glucose analog 2-(*N*-(7-Nitrobenz-2-oxa-1,3-diazol-4-yl)Amino)-2-Deoxyglucose (2-NBDG, Thermo Fisher Scientific). Cells were exposed to a 100 μM solution of 2-NBDG in glucose- and phenol red-free medium at the 3 undigested and digested NP concentrations and with an unexposed control. Each monolayer was exposed to 100 μL exposure solution. Samples from the basolateral chambers were taken at 10 different time points and placed in a black 96 well plate (Coring), and fluorescence was measured with a plate reader (Biotek Synergy 2, Winooski, VT) at an excitation/emission spectrum of 485/528 nm (Richter et al., 2018).

Blank wells that contained no cells were also subjected to the same treatment to ensure that the effects were not dependent on the interactions of the NP with the porous membranes or glucose analog. More information about experimental procedure and blank well results can be found in Supplementary Figure 1.

2.11 Fatty acid uptake

Cellular uptake studies of free fatty acids were performed in 24 well plates (Corning) using fluorescent BODIPY® 500/510 C1, C12 (4, 4-Difluoro-5-Methyl-4-Bora-3a, 4a-Diaza-s-Indacene-3-Dodecanoic Acid, ThermoFisher). These are intensely fluorescent fatty acid analogs that are metabolized in cells in a way that mimics natural lipids, making them very effective in tracing lipid uptake (Hansen et al., 2011). Stock solutions were prepared in 5 mmol/L ethanol solution, and stored at −20 °C. Caco-2/HT29-MTX co-cultures were rinsed after a 4 hour exposure to NP with 200 μL ice cold DMEM. The fluorescent fatty acid was added to the culture medium to obtain a final concentration of 50 μmol/L in DMEM, 200 μL was added to each well, and the plates were placed in the incubator at 37°C and 5% CO_2 for 10 minutes. After 10 minutes the medium was quickly replaced with regular DMEM and the cells were incubated for an additional hour. Fluorescence in each well was measured with a fluorescent plate reader (Biotek Synergy 2, excitation/emission, 490/530).

2.12 Intestinal Alkaline Phosphatase (IAP) activity assay

Co-cultures were seeded into 24 well plates and exposed to all undigested and digested NP concentrations for 4 hours. Following exposure, cells were rinsed with PBS and then 200 μL of 18 MΩ DI water was added to each well, plates were sealed using sealing film (Parafilm, Bemis NA), and then sonicated (VWR® Symphony™ Ultrasonic Cleaners, RF-48 W, 35k Hz operation frequency) for 5 minutes at room temperature. The cells were scraped from the bottom of the well and the lysate of each well was placed into a separate 1.5 mL centrifuge tubes.

A *p*-nitrophenyl phosphate (pNPP) solution was made by dissolving 1 Tris Buffer tablet and 1 pNPP tablet (Sigma Aldrich product T8915 and N9389, respectively) in 5 mL of 18 MΩ DI water. IAP hydrolyzes pNPP to *p*-nitrophenol, which turns bright yellow based on the concentration present. A 25 μL aliquot of cell lysate solution from each tube was added to a 96-well plate. Next, 85 μL of the pNPP solution was added to the wells and the plate was

incubated at room temperature for 1 hour wrapped in aluminum foil. The absorbance was read on a plate reader at 405 nm. The concentration of *p*-nitrophenol was determined with a standard curve. A Bradford assay (SigmaAldrich, St. Louis, MO) was performed using the same lysates to determine the amount of cell protein in mg/mL. A bovine serum albumin (BSA, ThermoFisher Scientific) standard curve was used to determine cell protein concentration.

2.13 Gene expression

Real-time PCR was used to examine changes in the expression of the genes encoding for DcytB, DMT1, HEPH, FPN1, FABP, FABP2, ZnT1, ZIP1, SGLT-1, GLUT2, IL-8, TNF-α, and NFκB. After NP exposure, the RNA was extracted from the cells using the RNeasy RNA extraction kit (Qiagen, Hilden, Germany). The RNA was converted to cDNA using the iScript cDNA synthesis kit (Bio-Rad, Hercules, CA). The resulting RNA was quantified using the NanoDrop 2000 (Thermo Fisher Scientific) to evaluate the ratio of absorbance at 260 and 280 nm. We considered samples with a ratio ~ 2 to be pure (Wilfinger et al., 1997) and diluted them to 30 ng/μL before converting to cDNA using the iScript cDNA synthesis kit (Bio-Rad, Hercules, CA). RNA was loaded into a Bio-Rad T100 thermal cycler for conversion to cDNA at a final volume of 20 μL. For real-time PCR measurements, 1 μL cDNA was added to a mixture of SsoAdvanced Universal SYBR Green Supermix (Bio-Rad), the corresponding primers, and water with 0.1% Diethyl pyrocarbonate (DEPC). qPCR was carried out for 50 cycles in a Bio-Rad MJ Mini thermal cycler. Gene expression was normalized to the expression of GADPH and compared with unexposed controls using the $2^{-\Delta\Delta Ct}$ method (Livak and Schmittgen, 2001). More details about the methodology, and the list of custom made primers (Thermo Fisher Scientific) and their sequences can be found in Guo et al. (Guo et al., 2017) and in Supplementary Table 1.

2.14 Scanning Electron Microscopy

Caco-2/HT29-MTX co-cultures were seeded at a density of 50,000 cells/cm^2 and grown for 2 weeks inside 6 well plates (Corning) on sterilized microscope cover slips coated with 8 μg/cm^2 collagen I. The monolayers were exposed to all undigested and digested concentrations of ZnO NP, and fixed after 4 hours in 4% paraformaldehyde in PBS. Next the cells were rinsed with PBS and dehydrated using an ethanol gradient (50, 75, 95,100 and 100%), transferred to hexamethyl disilizane (HMDS) and dried overnight (1:2 HMDS: Ethanol, 2:1 HMDS: Ethanol, 100% HMDS). The cover slips were removed from the 6 well plates and then mounted on SEM mounts (Ted Pella, Inc.), carbon coated, and viewed using a Zeiss Supra 55 Scanning Electron Microscope (Oberkochen, Germany) at 5 keV. 3 microscope slides per concentration were made, and 3 areas per sample were analyzed, resulting in n=9 replicates per concentration.

2.15 Statistical Analysis

In vitro results are expressed as mean ± standard deviation (SD). A one-way ANOVA with Tukey's post-test was used as an assessment between multiple groups. Gene expression changes were analyzed with a two-way ANOVA with Tukey's multiple comparison test. For the glucose transport studies, normality of distribution was determined with a D'Agostino & Pearson omnibus K2 test. Statistical significance was determined using a nonlinear

regression model with replicates test for lack of fit. Out of the models tested, the quadratic model was accepted as the best fit. Curve fits were compared using the Akaike's Information Criteria (AIC) from a quadratic model. Statistical analysis was performed using *Graphpad Prism 5* and samples were considered significant at $p<0.05$.

3. Results

3.1 Zn dose calculations.

Figure 1 shows the amount of Zn in different types food canned meats and vegetables, and the detailed data is found in Table 1 and Table 2. Table 1 shows the average Zn concentrations per sample. Table 2 shows the hydrated and dehydrated food sample weights. These data were used to determine the concentration of Zn per sample. If 12.6 g of hydrated tuna results in 5.3g in dry weight, then a whole serving of tuna (112g) would weigh ~ 47g after freeze-drying. Then by multiplying the amount of dehydrated sample times the mean concentration of Zn found in that sample we get the total amount of Zn per serving of canned food:

$$\frac{26.9 mg\ of\ Zn}{1 kg\ of\ freeze\ dried\ tuna} x\ 0.0471 kg\ of\ sample = 1.27\ mg\ Zn$$

For the asparagus:

$$\frac{66.7 mg\ of\ Zn}{1 kg\ of\ freeze\ dried\ tuna} x\ 0.0122 kg\ of\ sample = 0.813\ mg\ Zn$$

Therefore:

$$1.27\ mg\ Zn\ from\ a\ serving (one\ 4\ oz\ can)\ of\ tuna + 0.813\ mg\ of\ Zn\ from\ a\ serving\ of\ asparagus = 2.08\ mg\ Zn\ per\ two\ servings\ of\ canned\ food .$$

A serving of tuna plus a serving of asparagus has ~ 200 calories according to the nutrition labels; if a person consumes 1000 calories from canned food, this would result in a total of ~10 mg of Zn consumed from canned food. As shown in Figure 2, Zn content varies depending on the brand as well as the location of the food within the can. It is not clear if the variation in Zn content is due to manufacturing practices, the amount of time that the cans have been sitting on shelves, or the conditions they have been exposed to during transportation. This amount of Zn was recreated in the laboratory using 10 nm ZnO NP in powder form using the radius (5nm) and the density of ZnO (5.61g/cm^3) to find the weight of each NP. To determine the amount of NP per meal Equations 1-3 were used:

$$V = \frac{4}{3}\pi(5nm)^3 = 523.60\ \mathrm{nm}^3 / \mathrm{NP} \quad \text{Equation 1:}$$

$$\left(523.60\frac{nm^3}{NP}\right)\left(\frac{1x10^{-21}cm^3}{nm^3}\right)\left(\frac{5610mg}{cm^3}\right)=\frac{2.94x10^{-15}mg}{NP} \quad \text{Equation 2:}$$

$$One\ serving=(10mg)(\frac{1\,NP}{2.94x10^{-15}mg})=3.4x10^{15}\,NP\ per\ serving \quad \text{Equation 3:}$$

This amount of NP per serving was divided by the surface area of the small intestine ($2\times10^6 cm^2$) (DeSesso and Jacobson, 2001) resulting in $1.\times10^9$ NP/cm^2, which is the low dose. From this dose we determined a medium dose at 1×10^{11} NP/cm^2 and a high dose at 1×10^{13} NP/cm^2. These amounts of ZnO NP were weighed and suspended in cell media or digest at the established concentrations for all the experiments and referred to as undigested or digested low, medium, and high concentrations. These doses are comparable to doses used in similar studies looking at ZnO nanoparticle toxicity in Caco-2 cells (Abbott Chalew and Schwab, 2013; Chia and Leong, 2016; Heng et al., 2011; Song et al., 2014; Zijno et al., 2015).

3.2 Nanoparticle Characterization

Table 3 summarizes the size of the ZnO NP analyzed by TEM, SEM Nanosight and Zetasizer. All suspensions in this table were performed at a concentration of 0.1 mg/mL. Despite the sonication, ZnO NP persistently aggregate in water. We used TEM to characterize the morphology and size of NP, as well as their diffraction chemistry. Figure 2C shows a high magnification image of a single ZnO NP where the lattice fringe can be appreciated. The lattice fringe is defined as a periodic fringe in a TEM image formed by a transmitted wave exiting from a crystal and a diffracted wave from one lattice plane of the crystal (JEOL, n.d.). A more detailed measurement was performed using ImageJ, and we found the distance between the apparent ‘’lines” to be ~0.25 nm (SI Fig. 2). These measurements in the lattice fringe correspond to literature values for crystalline ZnO NP (Yan et al., 2003), meaning that the TEM images are of high resolution and quality. After we subjected these same NP to the *in vitro* digestion process or simply suspended them in DMEM, the ZnO were no longer found in nanoparticulate form and the Zn seemed to be distributed throughout the sample. A dark, thick “spread” or “blob” of material can be seen in some samples (Fig. 3D). Energy dispersive X-ray spectroscopy (EDS) confirm that these spreads are primarily composed of C, Ca, P, Cl, and O, but they also contain 1-3% Zn. This is evidence of the biotransformation that occurs after the NP reaches biological media, which is in agreement with dissolution experiments performed by Reed et al. (Reed et al., 2012) and evidence that the NP do not reach the small intestine in nanoparticulate form.

3.3 Cell Viability, Immunocytochemistry and Transepithelial Electrical Resistance.

Immunocytochemistry (ICC) was performed after ^{58}Fe and ^{67}Zn transport experiments at the control and low concentrations. We observed that when only ^{67}Zn isotope or the low concentration of Zn was added to the cells, the tight junctions were better delineated and

visible compared to the cells that were only treated with ^{58}Fe isotope and were therefore Zn deficient (Fig. 4A and B). After NP exposure, we observed a significant increase in the TEER of all concentrations of digested NP compared to the undigested NPs (Fig. 4C). For the cell viability study (Fig. 5C) we did not observe any significant difference between the control undigested NP and the low and medium ZnO NP doses for both undigested and digested NP. Only the high concentrations of ZnO NP (both undigested and digested) have a significantly higher percentage of live cells (Fig. 5A). As shown in Live/Dead fluorescent cell images (Fig. 6), it appears that there are more dead cells resulting from exposure to digests when compared to cells exposed to undigested NP, but this was independent of NP concentration. The raw fluorescence data of the viability assay (Fig. 5C) shows no significant difference between treatments except for the high digest, in which the fluorescence for live cells is significantly increased. The fluorescent microscope images also confirm these results (Fig. 6). In Figure 6 we can observe that there are more dead cells (red) in the digested NP treated cells than in the undigested NP treated cells, but overall there does not seem to be a decrease in living cells (green).

3.4 Effects of Zn NP on mineral and macronutrient transport.

In this study we assessed the effect of ZnO NP exposure on the absorption and transport of several essential nutrients. Transwell inserts (Corning, 2013) were used to determine the nutrients that were being transported from the apical to the basolateral chambers, which is representative of the transport from the small intestine into the bloodstream *in vivo*.

Fe and Zn are essential nutrients necessary for many biochemical reactions in the body. In this study, we observed a significant decrease of Fe transport at the highest doses of ZnO NP exposure (Fig. 7A). In the case of Zn, there was a significant decrease observed at the medium and high undigested and digested concentrations of ZnO NP compared to the control.

The effect of the ZnO NP on macronutrient transport was also studied. Glucose transport was significantly decreased with increasing addition of digested ZnO NP, but this effect was not observed with the undigested ZnO NP suspended in DMEM (Fig. 7B). In the case of lipids (another major category of macronutrient), a slight decrease was observed with the cells that were treated with undigested ZnO NP, but the decrease was not statistically significant (Fig. 6C).

3.5 Intestinal Alkaline Phosphatase.

IAP was decreased with the addition of undigested ZnO NP, while a slight increase was observed in the case of cells exposed to *in vitro* digested ZnO NP suspensions, but the changes were not statistically significant. The findings are summarized in Figure 8.

3.6 Gene expression

Table 4 shows significant changes in gene expression following the addition of ZnO NP to the *in vitro* model.

3.7 Scanning Electron Microscope

Analysis of the cell morphology using SEM demonstrated a lower cell area covered by microvilli in the cells exposed to the highest concentration of digested ZnO NP (Fig. 9), which was then quantified using ImageJ to measure the percent area of microvilli. (Supplemetary Fig. 3).

4 Discussion

4.1 Zn dose calculations.

A primary goal of this study was to estimate physiologically relevant NP exposure doses, but we cannot determine if the cans contain ZnO in nanoparticulate form because this information is not disclosed. In addition, we cannot ascertain that all of the ZnO is coming from the can, given that we do not know all of the steps that go into the packaging procedure of these foods. However, the National Institutes of Health (NIH, n.d.) have published a list of foods that are naturally high in Zn, and they primarily include seafood. In this list, tuna, which is the food that we found to be highest in Zn, is not included. The United States Department of Agriculture Food Composition Databases (USDA, n.d.) has a list of foods that can be searched by a specific nutrient content. We used this database, and the reported amounts for Zn in our studies is more than 8 times the amount listed in the database for raw tuna. This is why we made the inference that the Zn content we found with ICP is coming from the cans, and not from the food itself. In addition, there have been previous studies performed looking at the amount of Zn and other minerals and metals in seafood, but none of these found a Zn amount higher than the amount found in this study. Work done in 1995 found 16 mg/kg in canned tuna using Flame Atomic Absorption Spectroscopy (Tahán et al., 1995). A study done by Celik et al. found that the amount of Zn in canned tuna in the Turkish market was more than twice as high the amount we found in local supermarkets (Celik and Oehlenschlager Jorg, 2007). Another study found that on average, fresh tuna in the French fish markets contains 4.35 mg/kg of Zn (Guérin et al., 2011), which less than a fifth of what we found in canned tuna in a US supermarket. All of this variation in quantification of Zn was a motivation for us to quantify the amount of Zn using ICP for our studies. And although we cannot determine if all of the Zn comes from the food or the can, a consumer who ingests tuna from a can will still be exposed to this amount of Zn, and therefore the concentration is physiologically relevant. If we consider that in addition to canned food, a consumer could take Zn supplements that are readily available in the supermarket, that could increase the amount of Zn consumed to more than 100 mg (“Zinc,” n.d.).

4.2 Nanoparticle Characterization

A possible explanation of the loss of the nanoparticulate form shown in Figure 3 is that the Zn^{2+} is being complexed with organic compounds found in the DMEM of the undigested suspensions and the enzymes and salts containing digested NP suspensions. Zn^{2+} is the only valence state that exists in living organisms (Krężel and Maret, 2016). About 10% of human proteins use Zn for catalysis and structure, and these Zn molecules remain bound through the protein’s lifetime, however in the case of other proteins, Zn^{2+} binding is reversible and dynamic, responding to the cell’s requirement for signaling, transport, regulation, storage,

among other functions (Krężel and Maret, 2016). The mobility of these unbound Zn^{2+} ions has not been thoroughly studied. Zn^{2+} has a high affinity to thiol groups present in amino acids contained in the DMEM. This leads us to infer that complexes with amino acids are being formed, as well as other complexes such as $ZnCl_2$ and $ZnCO_3$. Similar predictions were done by Reed et al. by performing a simulation using Visual MINTEQ version 3.0 using a concentration similar to our high dose in DMEM (Reed et al., 2012).

The study by Reed et al. of ZnO NP in DMEM suggested that, depending on the starting concentration of ZnO NP, they dissolve and form complex ligands (Reed et al., 2012). This study observed that in concentrations above 5.5×10^{-3}mg/mL, more $ZnCO_3$ is formed and less Zn^{2+} is released, but in lower concentrations, ZnO NP fully dissolve in DMEM. Immediate Zn^{2+} dissolution of approximately 10 mg/mL was observed, and after 1446 hours, the Zn concentration exceeded 34 mg/mL, compared to nanopure water, which reached only 7.4 mg/mL. Reed et al. used an excess solution of 0.1 mg/mL, which is very close to our highest dose (0.097 mg/mL). From this study, we can infer that our highest solutions would reach approximately 12.5 mg/mL dissolution, but not complete dissolution. This was also observed in some of the highest DMEM and digest samples in which small nanoparticle aggregates were found (Fig. 3). At the lower doses the NP would completely dissolve into Zn^{2+} in this medium according to Reed et al. (Reed et al., 2012). but more information is needed to support this claim, since microscope techniques cannot show the full extent of dissolution.

If the ZnO NP readily dissolve, this could mean that the Zn^{2+} could be transported more easily by serum proteins to which Zn could be complexed (Scott and Bradwell, 1983) and therefore reach the bloodstream. A similar phenomenon was observed in Chung et al.(Chung et al., 2013), where rats were exposed to different concentrations of ZnO NP, that were later found in blood samples. Also, after being chronically exposed to several concentrations of ZnO NP, Zn plasma levels were elevated and did not return to normal after 24 hours (Chung et al., 2013). Zn has also been shown to accumulate in the kidney and the liver and to appear in feces and urine after prolonged exposure, which resulted in decreased Fe levels (Bergin and Witzmann, 2013; Srivastav et al., 2016).

4.3 *In vitro* digestion

It is important to consider the size-dependent effects of ZnO NP, however, the NP will very likely undergo transformation before reaching the cells when they are dissolved in cell culture medium, or when they undergo a digestion process. One study done in marine organisms found that the ZnO NP formed aggregates that ended up being larger than the non-nano ZnO in seawater (Wong et al., 2010). In terms of toxicity, ZnO NP were shown to be more toxic to algae than to fish and crustaceans when compared with bulk ZnO, implying that toxicity of Zn is complicated and varies by organisms. In a study done in human monocytes, it was found that 100 nm ZnO NP induced more inflammatory responses and decreased phagocytic capability compared to 5μm particles (Sahu et al., 2014). In another done in lung epithelial cells, results showed that no significant difference was seen in the toxicity caused by 70nm ZnO NP compared to 420 nm ZnO NP (Lin et al., 2009).

Reed et al. performed experiments with bulk ZnO in DMEM with BSA, and their results show very similar dissolution to nano ZnO. This may explain why some studies have shown that using bulk ZnO and comparing its toxicity with nano ZnO often results in similar effects (Reed et al., 2012). To make the experiments more physiologically relevant, we subjected the NP to an *in vitro* digestion process that contained salts and enzymes present in the stomach, and the pH was adjusted corresponding to the stages of digestion. ZnO is amphoteric and therefore it is very reactive to pH changes, making it behave differently in complex media. We observed this behavior when the nanoparticles appeared to dissolve after adding the HCl to lower the pH, we were able to see a visual change in the colloidal suspension of NP to a more clarified solution. The dissolution of the nanoparticles was later confirmed with TEM (Fig. 3). David et al. demonstrated that a decrease in pH of only 0.15 doubles the concentration of Zn^{2+} released in a buffered solution (David et al., 2012). Reed et al. suggested that the addition of BSA causes higher solubility in ZnO NP likely because of the protein corona effect (Reed et al., 2012). Our experiments show that the NP are not likely to reach the cells in nanoparticulate form after undergoing a digestion process.

4.4 ZnO NP Effects on Cell Viability and Tight Junction Functionality.

The small intestine is formed by several types of cells joined by intercellular junctional structures known as tight junctions (TJ) that control intestinal permeability. The majority of these cells (80%) are absorptive enterocytes that form the intestinal epithelium (Ulluwishewa et al., 2011).

ICC of the TJ protein occludin in addition to transepithelial electrical resistance (TEER) measurements are well established methods for evaluating tight junction functionality and monolayer integrity (Narai et al., 1997). An increase of permeability of the TJ is considered a sub-lethal toxic effect given that it disrupts barrier function of the epithelium. A decrease in permeability also allows small molecules to flow freely from the intestinal lumen into the bloodstream (Narai et al., 1997; Ranaldi et al., 2002). TEER is an indicator of how strong the tight junctions are, and a reduced TEER normally indicates ‘leaky’ junctions, which in the small intestine is very detrimental and associated with diseases such as irritable bowel syndrome and Crohn's disease (Liu et al., 2005).

Cell death is likely due to the high amount of salts and enzymes from the *in vitro* digestion components and not because of the NP, given that the highest DMEM NP concentration had the same viability as the DMEM control (Fig. 5C). The increase in TEER is due to a strengthening of the tight junctions caused by exposure to Zn. Previous studies with piglets have demonstrated that supplementing the pig’s diet with a high amount of ZnO (2000mg/kg or more) enhances occludin and other TJ proteins such as ZO-1 and increases the TEER of the small intestine (Hu et al., 2013; Kelleher and Lönnerdal, 2006; Lind et al., 2003; Wang et al., 2013; Zhang and Guo, 2009). It is also widely accepted that zinc deficiency will affect the quality and strength of tight junctions, as well as delocalization of TJ proteins, but the mechanism is not well understood. Therefore, although ZnO NP have been observed to cause damage to certain organisms (Vandebriel and De Jong, 2012) the mechanism by which they do so is probably not related to cellular TJ damage.

4.5 ZnO NP Effects on Nutrient Transport

Absorption of nutrients is the single most important function of the small intestine. This occurs by the formation of an electrochemical gradient across the apical and basolateral sites of the monolayer that provides energy for numerous chemical reactions. We assessed the effect of ZnO NP exposure on the absorption and transport of several essential nutrients. Transwell inserts (Corning, 2013) were used to determine the nutrients that were being transported from the apical to the basolateral chambers, which is representative of transport into the bloodstream *in vivo*, and also measured the gene expression of important cellular transporters (summarized in Table 4). Other studies have been done to determine the effect of ZnO NP on cell viability, ROS formation, and pro-inflammatory responses(Abbott Chalew and Schwab, 2013; Kang et al., 2013; Setyawati et al., 2015; Zödl et al., 2003). This is why in addition to studying the toxic effects of ZnO NP on intestinal cells, we measured the functional effects of ZnO NP exposure, specifically the effects on micro and macronutrient absorption.

Fe is one of the most essential minerals in the body, as well as one of the best characterized. Fe deficiency causes anemia, which results in a lack of red blood cells and decreased oxygen transport, and defects in iron metabolism result in serious diseases (Lind et al., 2003). Studies have demonstrated decreased hemoglobin, ferritin levels, and Fe absorption caused by Zn supplementation, but the mechanism is not thoroughly understood (Arredondo et al., 2006; Eide, 2006; Espinoza et al., 2012). This study investigated the effect of ZnO NP doses on Fe transport in the small intestine.

There was a decrease in Fe transport at the low, physiologically relevant dose, which is in agreement with the studies showing that Zn supplementation can cause decreased Fe absorption (Arredondo et al., 2006; Eide, 2006; Espinoza et al., 2012), however at the low dose these changes are not statistically significant (Fig 7A). The most significantly different treatment was the high concentration of NP in MEM, which showed approximately 75% lower Fe transport than the untreated control (Fig. 7A). In the case of Zn, we did not observe such dramatic differences. We also examined the gene expression of Fe transporters to understand the changes in Fe transport caused by excess Zn. One explanation for the observed decrease in the high dose of low-mineral MEM is that Zn^{2+} and Fe^{2+} can both be transported by the divalent metal transporter 1 (DMT1) (Collins, 2006) and an excess of Zn^{2+} may have competitively inhibited the transport of $Fe.^{2+}$ Our analysis of DMT1 showed an increase in DMT1 activity at our low digest dose, but not in the low DMEM dose. This is most likely due to greater Zn^{2+} ion release in digest conditions. In general, a dose dependent increase of DMT1 was seen for our medium and high dose, which is consistent with research that has shown that rats that have been deprived of iron highly upregulate DMT1 as well as the duodenal cytochrome B (Dcytb) (Collins, 2006). Another study performed in humans demonstrated that DMT1, Dcytb, and hephaestin (HEPH), which are iron transporters, are upregulated in patients with hemochromatosis and iron deficiency (Zoller et al., 2003). In our studies, we observed an increase in the expression of HEPH of the cells exposed to low and medium concentrations of ZnO NP in DMEM, but it was not statistically significant. A different study proposes that Zn supplementation causes Fe intestinal retention by decreasing the amount of Ferroportin (FPN) (Kelleher and Lönnerdal, 2006), which

recirculates the Fe into the bloodstream in the basolateral side of the epithelium. In this study, we observed a decrease in FPN1 for the highest NP dose, but it was not statistically significant.

In the case of Zn transport, the digest containing a low dose of ZnO NP resulted in significantly higher ^{67}Zn transport than the medium and high dose digests. As demonstrated by Reed et al.,(Reed et al., 2012) saturated zinc concentration may cause Zn to precipitate into $ZnCO_3$ leaving it unavailable for cells to absorb. Gene expression shows an increase in the Zip1 transporter protein gene expression for all doses of NP in DMEM and digests, but this increase was not statistically significant. Zip1 is the major zinc apical transporter in the small intestine (Eide, 2006), and it has been shown that increasing dietary zinc consumption leads to an increase of the expression of Zip1 in the small intestine (Méndez et al., 2014). ZnT1 has been observed to increase with rising zinc levels, which might be to avoid excessive accumulation of zinc in the cytosol by removing zinc through the basolateral membrane of the small intestine (Cousins and McMahon, 2000; Palmiter and Findley, 1995). We observed that ZnT1 was significantly upregulated for the high dose in DMEM (Table 4). Zinc excess can have effects on human health. Previous work showed that Zn and Cu readily affect the transport of Zn, and that Fe excess can inhibit Cu uptake, but not Zn uptake. When the 3 metals are fed together in the same ratio, Fe and Cu transport are inhibited by approximately 40%. This suggests that zinc readily inhibits other metals when administered in excess (Arredondo et al., 2006).

Macronutrients are needed in large amounts in the human body to provide energy for all chemical reactions, and they are divided into carbohydrates, fats and proteins. We examined carbohydrates because they are the most widely consumed and fats because they have the highest caloric density. Carbohydrates are the main source of human energy and the easiest for the intestine to absorb (Jéquier, 1994). ZnO nanoparticles decreased the absorption of glucose, especially in the digests, in a dose-dependent manner (Fig. 7B).

There is a link between zinc deficiency and diabetes, and several studies in rats show that the introduction of Zn alone can dramatically improve the effect of streptozotocin injection in mice (Alkaladi et al., 2014; Chen et al., 1998). This might be because of an important role of Zn in the insulin hormonal cascade, and there are also theories that say that Zn can act as insulin in certain conditions, resulting in a reduction of blood glucose (O'Halloran et al., 2013). Early studies proposed that Zn binds to the sodium-glucose transporter 1 (SGLT1) and reduces the affinity of glucose to (SGLT) (Lyall et al., 1979; Rodríguez-Yoldi et al., 1995; Watkins et al., 1989). Expert opinion states that inhibition of SGLT1 can reduce the absorption of glucose in the intestine (Song et al., 2016). Our gene expression studies revealed a decrease in SGLT1 for most treatments, but results were not statistically significant. This is one mechanism that can explain the reduction of glucose in the cells exposed to the digests. One of the already mentioned studies theorizes that Zn inhibits the activity of Na^+/K^+-ATPase of the cells, which affects the Na dependent transport of D-galactose (Rodríguez-Yoldi et al., 1995).

In the case of fatty acid uptake, the data show a slight decrease in fatty acid uptake, however no statistical significant difference was observed for any of the concentrations (Fig. 7C).

Zinc supplementation has been associated with reduced total cholesterol levels, LDL cholesterol and triglycerides in some cases (Gunasekara et al., 2011), however the mechanisms are not completely understood, and there is conflicting information regarding the effect of Zn on lipid absorption in the human body (Jayawardena et al., 2012). One study performed in Zn deficient rats showed a downregulation of transcription levels of proteins involved in the metabolism of lipids, and an upregulation of proteins needed for fatty acid synthesis (tom Dieck et al., 2005).

4.6 Injury and stress responses caused by ZnO NP exposure.

Scanning electron microscopy of the cell co-cultures demonstrated that higher concentrations of digested ZnO NP caused disruption of the brush border membrane. All digest we statistically significant decrease in surface area of microvilli when compared to their DMEM counterparts (SI Fig. 3). When comparing the DMEM samples to the digests samples, there was a statistically significant decrease in the surface area covered by microvilli in the digest-exposed samples (SI Fig. 3), which could explain the decrease in glucose absorption.

Koeneman et al. (2010) and Guo et al. (2017 and 2018) demonstrated that exposure to TiO_2 and SiO_2 NP resulted in a decrease in absorptive cell microvilli (Guo et al., 2018, 2017; Koeneman et al., 2010). To our knowledge, this is the first demonstration of evidence that suggests that digested ZnO NP may alter the microvilli in the Caco-2/HT29-MX co-cultures. This explains some of the micro and macronutrient alterations that were observed in the data explained previously. A decrease in the amount of microvilli decreases absorptive surface area, which likely causes decreased uptake and transport of nutrients.

Intestinal Alkaline Phosphatase (IAP) is an enzyme that is present in the liver, bones, kidneys and the small intestine. The main role of IAP is to dephosphorylate complex ligands from microbes and therefore keep the intestine protected, primarily from gram negative bacteria (Goldberg et al., 2008). Other studies in Caco-2 cells reveal that IAP also has an important role in the enhancement of tight junctions, thereby reducing permeability (Liu et al., 2015). It is important to note that Zn deficiency has shown to cause decreased IAP activity, which shows that along with the increased TJ functionality, that there are several pathways of Zn protection in the small intestine (Lallès, 2014). IAP can protect the intestine from several forms of insult. When there is an injury in the intestine, IAP increases to protect the gut from incoming bacteria, and if the intestine becomes too acidic, IAP increases the pH of the intestinal lumen by upregulating sodium bicarbonate secretion (Mizumori et al., 2009). Although there was damage to the microvilli of the cells, our studies did not show a significant difference in IAP activity caused by the addition of ZnO NP (Fig. 8). In addition, we observed upregulation in the proinflammatory genes TNFα and NFκB for the cells exposed to digests, but these were not significantly different. There was only one pro-inflammatory response, indicated by the upregulation of IL8 at the highest ZnO concentration in DMEM. These responses can be caused by oxidative stress (Kang et al., 2013; Moos et al., 2011).

We should consider that ZnO NP can have negative effects in certain cells more than in others. Work by Henley et al. have shown selective toxicity of ZnO in cancerous cells when

compared with healthy cells (Hanley et al., 2008). In addition, earlier work by Ng et al. and Setyawati et al. demonstrated that a cell's genetic makeup is more determinant when assessing toxicity of ZnO NP than the NP themselves (Ng et al., 2011; Setyawati et al., 2013). Roselli et al. has revealed that the same Zn NP have different toxicities in bacteria compared to human T cells (Roselli et al., 2003). Some studies suggest that ZnO can protect the intestine from certain diseases, and that it might selectively target the harmful bacteria. Rosselli et al. suggested that this may be due to the ZnO antimicrobial effects that can reduce the damage in the intestine from *E. coli* (Roselli et al., 2003), although this would not explain the increased tight junction functionality. Perhaps in the case of small intestine, Zn can cause more benefit than harm, but the fact that it is readily dissolving into ions may mean that Zn can very easily travel to parts of the body where it might not be as beneficial, such as in the lungs (Cho et al., 2011; Jachak et al., 2012).

Perhaps the most important highlight is the challenge of complex mineral interactions in the intestine. It seems that the balance can be very easily disturbed by simply adding too much of one mineral compared with another. Zn is necessary for more than 300 biological processes in the body (Roohani et al., 2013), but Fe and Cu are equally important, compete for the same transporters, and they seem to interact in a very complex manner. We only used the canned food doses as a reference for a potentially realistic dose. We cannot say for certain that these are NP, this is due to the lack of information from manufacturers. The FDA does not require manufacturers to include the amount of NP or their full characterization profile.

Conclusions

This study highlights the importance of assessing the safety of food products that contain NP. The first step is determining the amount of nanomaterials that are potentially leached into the food in order to create physiologically relevant experiments that can thoroughly assess the risk of human exposure to NP. In this study, we estimated ZnO NP doses by measuring the amount of Zn in canned food, and determined that the ZnO NP would likely dissolve after ingestion. We also concluded that the uptake and transport of nutrients is affected by the amounts of zinc that may be consumed from cans. At physiologically relevant concentrations, glucose absorption was significantly reduced after the addition of digested NP, as well as gene expression of its basolateral transporter GLUT2. Cell microvilli were also affected by the digested ZnO NP, reducing the surface area available for absorption. At higher ZnO NP concentrations, pro-inflammatory responses were observed with the upregulation of pro-inflammatory genes, and there was a decrease in iron transport. Overall, these results show that there are significant changes caused by NP exposure in a cell culture model of the small intestine, and that evaluating the cytotoxicity of nanoparticles in food packaging is important for consumer safety. An *in vitro* model with gut functional assays provides a rapid method for assessing the effects of ingested NP on nutrient absorption and enzyme function.

Supplementary Material

Refer to Web version on PubMed Central for supplementary material.

Acknowledgements

This work was supported by the National Institutes of Health (1R15ES022828) and the Mexican National Council of Science and Technology (CONACyT) Fellowship. This work shared facilities and was supported by the Virginia Tech National Center for Earth and Environmental Nanotechnology Infrastructure (NanoEarth), a member of the Nanotechnology Coordinated Infrastructure (NNCI), supported by NSF (ECCS 1542100). We would also like to acknowledge Mridu Malik and Andrew Goldman for assistance with experimental methods and result analysis.

References

Abbott Chalew TE, Schwab KJ, 2013 Toxicity of commercially available engineered nanoparticles to Caco-2 and SW480 human intestinal epithelial cells. Cell Biol. Toxicol 29, 101–116. 10.1007/s10565-013-9241-6 [PubMed: 23468361]

Alkaladi A, Abdelazim AM, Afifi M, 2014 Antidiabetic activity of zinc oxide and silver nanoparticles on streptozotocin-induced diabetic rats. Int. J. Mol. Sci 15, 2015–2023. 10.3390/ijms15022015 [PubMed: 24477262]

Alo DC, 1965 Sulfur Staining in canned foods: its diagnosis and prevention. Anti-Corrosion Methods Mater. 12, 17.

Arredondo M, Martínez R, Núñez MT, Ruz M, Olivares M, 2006 Inhibition of iron and copper uptake by iron, copper and zinc, in: Biological Research. pp. 95–102. 10.4067/S0716-97602006000100011 [PubMed: 16629169]

Auffan M, Rose J, Bottero JY, Lowry GV, Jolivet JP, Wiesner MR, 2009 Towards a definition of inorganic nanoparticles from an environmental, health and safety perspective. Nat. Nanotechnol 4, 634–641. 10.1038/nnano.2009.242 [PubMed: 19809453]

Barret DM, Somogyi L, Ramaswamy H, 2005 Processing Fruits: Science and technology, Processing Fruits:Science and Technology. 10.1201/9781420040074.ch20

Bergin IL, Witzmann F. a, 2013 Nanoparticle toxicity by the gastrointestinal route: evidence and knowledge gaps. Int. J. Biomed. Nanosci. Nanotechnol 3, 1–46. 10.1504/IJBNN.2013.054515

Celik U, Oehlenschlager Jorg, 2007 High contents of cadmium , lead , zinc and copper in popular fishery products sold in Turkish supermarkets. Food Control 18, 258–261. 10.1016/j.foodcont.2005.10.004

Chaudhry Q, Scotter M, Blackburn J, Ross B, Castle L, Aitken R, Watkins R, 2008 Applications and implications of nanotechnologies for the food sector. Food Addit. Contam. Part A. Chem. Anal. Control. Expo. Risk Assess 25, 241–258. 10.1080/02652030701744538

Chen MD, Liou SJ, Lin PY, Yang VC, Alexander PS, Lin WH, 1998 Effects of zinc supplementation on the plasma glucose level and insulin activity in genetically obese (ob/ob) mice. Biol. Trace Elem. Res 61, 303–11. 10.1007/BF02789090 [PubMed: 9533568]

Chia SL, Leong DT, 2016 Reducing ZnO nanoparticles toxicity through silica coating. Heliyon 2. 10.1016/j.heliyon.2016.e00177

Chia SL, Tay CY, Setyawati MI, Leong DT, 2015 Biomimicry 3D gastrointestinal spheroid platform for the assessment of toxicity and inflammatory effects of zinc oxide nanoparticles. Small 11, 702–712. 10.1002/smll.201401915 [PubMed: 25331163]

Cho W-S, Duffin R, Howie SE, Scotton CJ, Wallace WA, MacNee W, Bradley M, Megson IL, Donaldson K, 2011 Progressive severe lung injury by zinc oxide nanoparticles; the role of Zn2+ dissolution inside lysosomes. Part. Fibre Toxicol. 8, 27 10.1186/1743-8977-8-27

Chung HE, Yu J, Baek M, Lee JA, Kim MS, Kim SH, Maeng EH, Lee JK, Jeong J, Choi SJ, 2013 Toxicokinetics of zinc oxide nanoparticles in rats, in: Journal of Physics: Conference Series. 10.1088/1742-6596/429/1/012037

Collins JF, 2006 Gene chip analyses reveal differential genetic responses to iron deficiency in rat duodenum and jejunum, in: Biological Research. pp. 25–37. [PubMed: 16629162]

Corning, 2013 Transwell ® Permeable Supports Selection and Use Guide [WWW Document]. URL http://csmedia2.corning.com/LifeSciences/Media/pdf/transwell_guide.pdf

Cousins RJ, McMahon RJ, 2000 Integrative aspects of zinc transporters. J. Nutr 130, 1384S–7S. [PubMed: 10801948]

David CA, Galceran J, Rey-Castro C, Puy J, Companys E, Salvador J, Monné J, Wallace R, Vakourov A, 2012 Dissolution kinetics and solubility of ZnO nanoparticles followed by AGNES. J. Phys. Chem. C 116, 11758–11767. 10.1021/jp301671b

DeSesso JM, Jacobson CF, 2001 Anatomical and physiological parameters affecting gastrointestinal absorption in humans and rats. Food Chem. Toxicol 39, 209–228. 10.1016/S0278-6915(00)00136-8 [PubMed: 11278053]

Eide DJ, 2006 Zinc transporters and the cellular trafficking of zinc. Biochim. Biophys. Acta - Mol. Cell Res 10.1016/j.bbamcr.2006.03.005

Espinoza A, Le Blanc S, Olivares M, Pizarro F, Ruz M, Arredondo M, 2012 Iron, copper, and zinc transport: Inhibition of divalent metal transporter 1 (DMT1) and human copper transporter 1 (hCTR1) by shRNA. Biol. Trace Elem. Res 146, 281–286. 10.1007/s12011-011-9243-2 [PubMed: 22068728]

Espitia PJP, Otoni CG, Soares NFF, 2016 Zinc Oxide Nanoparticles for Food Packaging Applications. Antimicrob. Food Packag 425–431. 10.1016/B978-0-12-800723-5.00034-6

Espitia PJP, N. de F.F. Soares, J.S. dos R. Coimbra, de Andrade NJ, Cruz RS, Medeiros EAA, 2012 Zinc Oxide Nanoparticles: Synthesis, Antimicrobial Activity and Food Packaging Applications. Food Bioprocess Technol. 10.1007/s11947-012-0797-6

Fröhlich EE, Fröhlich E, 2016 Cytotoxicity of nanoparticles contained in food on intestinal cells and the gut microbiota. Int. J. Mol. Sci 10.3390/ijms17040509

García-Rodríguez A, Vila L, Cortés C, Hernández A, Marcos R, 2018 Exploring the usefulness of the complex in vitro intestinal epithelial model Caco-2/HT29/Raji-B in nanotoxicology. Food Chem. Toxicol 113, 162–170. 10.1016/j.fct.2018.01.042 [PubMed: 29421767]

Glahn RP, Lee OA, Yeung A, Goldman MI, Miller DD, 1998 Caco-2 cell ferritin formation predicts nonradiolabeled food iron availability in an in vitro digestion/Caco-2 cell culture model. J. Nutr 128, 1555–61. [PubMed: 9732319]

Goldberg RF, Austen WG, Jr., Zhang X, Munene G, Mostafa G, Biswas S, McCormack M, Eberlin KR, Nguyen JT, Tatlidede HS, Warren HS, Narisawa S, Millan JL, Hodin RA, 2008 Intestinal alkaline phosphatase is a gut mucosal defense factor maintained by enteral nutrition. Proc Natl Acad Sci U S A 105, 3551–3556. 10.1073/pnas.0712140105 [PubMed: 18292227]

Groh KJ, Geueke B, Muncke J, 2017 Food contact materials and gut health: Implications for toxicity assessment and relevance of high molecular weight migrants. Food Chem. Toxicol 109, 1–18. 10.1016/j.fct.2017.08.023 [PubMed: 28830834]

Guérin T, Chekri R, Vastel C, Sirot V, Volatier J, Leblanc J, Noël L, 2011 Determination of 20 trace elements in fish and other seafood from the French market 127, 934–942. 10.1016/j.foodchem.2011.01.061

Gunasekara P, Hettiarachchi M, Liyanage C, Lekamwasam S, 2011 Effects of zinc and multimineral vitamin supplementation on glycemic and lipid control in adult diabetes. Diabetes, Metab. Syndr. Obes. Targets Ther 4, 53–60. 10.2147/DMSO.S16691

Guo Z, Martucci N, Liu Y, Yoo E, Tako E, Mahler G, 2018 Silicon dioxide nanoparticle exposure affects small intestine function in an in vitro model. Nanotoxicology Unpublished.

Guo Z, Martucci NJ, Moreno-Olivas F, Tako E, Mahler GJ, 2017 Titanium dioxide nanoparticle ingestion alters nutrient absorption in an in vitro model of the small intestine. NanoImpact 5, 70–82. 10.1016/j.impact.2017.01.002 [PubMed: 28944308]

Hackenberg S, Scherzed A, Technau A, Kessler M, Froelich K, Ginzkey C, Koehler C, Burghartz M, Hagen R, Kleinsasser N, 2011 Cytotoxic, genotoxic and pro-inflammatory effects of zinc oxide nanoparticles in human nasal mucosa cells in vitro. Toxicol. Vitr 25, 657–663. 10.1016/j.tiv.2011.01.003

Hanley C, Layne J, Punnoose A, Reddy KM, Coombs I, Coombs A, Feris K, Wingett D, 2008 Preferential killing of cancer cells and activated human T cells using ZnO nanoparticles. Nanotechnology 19 10.1088/0957-4484/19/29/295103

Hansen GH, Rasmussen K, Niels-Christiansen L-L, Danielsen EM, 2011 Dietary free fatty acids form alkaline phosphatase-enriched microdomains in the intestinal brush border membrane. Mol. Membr. Biol 28, 136–144. 10.3109/09687688.2010.542552 [PubMed: 21166483]

Hansson GC, 2012 Role of mucus layers in gut infection and inflammation. Curr. Opin. Microbiol 10.1016/j.mib.2011.11.002

Hekal IM, Erlandson PM, 1981 US Pat. US4615924A.

Heng BC, Zhao X, Tan EC, Khamis N, Assodani A, Xiong S, Ruedl C, Ng KW, Loo JSC, 2011 Evaluation of the cytotoxic and inflammatory potential of differentially shaped zinc oxide nanoparticles. Arch. Toxicol 85, 1517–1528. 10.1007/s00204-011-0722-1 [PubMed: 21656222]

Hillyer JF, Albrecht RM, 2001 Gastrointestinal persorption and tissue distribution of differently sized colloidal gold nanoparticles. J. Pharm. Sci 90, 1927–1936. 10.1002/jps.1143 [PubMed: 11745751]

Hu CH, Xiao K, Song J, Luan ZS, 2013 Effects of zinc oxide supported on zeolite on growth performance, intestinal microflora and permeability, and cytokines expression of weaned pigs. Anim. Feed Sci. Technol 181, 65–71. 10.1016/j.anifeedsci.2013.02.003

Invitrogen Molecular Probes, 2005 LIVE/DEAD Viability/Cytotoxicity Kit for mammalian cells [WWW Document]. URL https://www.thermofisher.com/order/catalog/product/L3224

Jachak A, Lai SK, Hida K, Suk JS, Markovic N, Biswal S, Breysse PN, Hanes J, 2012 Transport of metal oxide nanoparticles and single-walled carbon nanotubes in human mucus. Nanotoxicology 6, 614–622. 10.3109/17435390.2011.598244 [PubMed: 21800953]

Jayawardena R, Ranasinghe P, Galappatthy P, Malkanthi R, Constantine G, Katulanda P, 2012 Effects of zinc supplementation on diabetes mellitus: a systematic review and meta-analysis. Diabetol. Metab. Syndr 4, 13 10.1186/1758-5996-4-13 [PubMed: 22515411]

JEOL, n.d. Glossary of TEM terms: Lattice Fringe [WWW Document]. URL https://www.jeol.co.jp/en/words/emterms/search_result.html?keyword=latticefringe

Jéquier E, 1994 Carbohydrates as a source of energy, in: American Journal of Clinical Nutrition. p. 682S–685S. [PubMed: 8116550]

Kalberg VN, 1951 US Pat. 2561379 A.

Kang T, Guan R, Chen X, Song Y, Jiang H, Zhao J, 2013 In vitro toxicity of different-sized ZnO nanoparticles in Caco-2 cells. Nanoscale Res. Lett 8 10.1186/1556-276X-8-496

Kelleher SL, Lönnerdal B, 2006 Zinc supplementation reduces iron absorption through age-dependent changes in small intestine iron transporter expression in suckling rat pups. J. Nutr 136, 1185–1191. [PubMed: 16614402]

Koeneman BA, Zhang Y, Westerhoff P, Chen Y, Crittenden JC, Capco DG, 2010 Toxicity and cellular responses of intestinal cells exposed to titanium dioxide. Cell Biol. Toxicol 26, 225–238. 10.1007/s10565-009-9132-z [PubMed: 19618281]

Krężel A, Maret W, 2016 The biological inorganic chemistry of zinc ions. Arch. Biochem. Biophys 611, 3–19. https://doi.Org/10.1016/j.abb.2016.04.010 [PubMed: 27117234]

Kumar KKV, Karnati S, Reddy MB, Chandramouli R, 2010 Caco-2 cell lines in drug discovery- an updated perspective. J. basic Clin. Pharm 1, 63–9. [PubMed: 24825967]

Lallès J-P, 2014 Intestinal alkaline phosphatase: novel functions and protective effects. Nutr. Rev 72, 82–94. 10.1111/nure.12082 [PubMed: 24506153]

Lesuffleur T, Barbat A, Dussaulx E, Zweibaum A, 1990 Growth Adaptation to Methotrexate of HT-29 Human Colon Carcinoma Cells Is Associated with Their Ability to Differentiate into Columnar Absorptive and Mucus-secreting Cells. Cancer Res. 50, 6334–6343. [PubMed: 2205381]

Lin W, Xu Y, Huang CC, Ma Y, Shannon KB, Chen DR, Huang YW, 2009 Toxicity of nano- and micro-sized ZnO particles in human lung epithelial cells. J. Nanoparticle Res. 11, 25–39. 10.1007/s11051-008-9419-7

Lind T, Lönnerdal B, Stenlund H, Ismail D, Seswandhana R, Ekström EC, Persson LA, 2003 A community-based randomized controlled trial of iron and zinc supplementation in Indonesian infants: interactions between iron and zinc. Am. J. Clin. Nutr 77, 883–890. [PubMed: 12663287]

Liu J, Hu J, Liu M, Cao G, Gao J, Luo Y, 2016 Migration and characterization of nano-zinc oxide from polypropylene food containers. Am. J. Food Technol 11, 159–164. 10.3923/ajft.2016.159.164

Liu W, Hu D, Huo H, Zhang W, Adiliaghdam L, Morrison S, Ramirez JM, Gul SS, Hamarneh SR, Hodin RA, 2015 Intestinal Alkaline Phosphatase Regulates Tight Junction Protein Levels. J. Am. Coll. Surg 222, 1009–1017. https://doi.Org/10.1016/j.jamcollsurg.2015.12.006 [PubMed: 27106638]

Liu Z, Li N, Neu J, 2005 Tight junctions, leaky intestines, and pediatric diseases. Acta Pædiatrica 94, 386–393. 10.1080/08035250410023304

Livak KJ, Schmittgen TD, 2001 Analysis of Relative Gene Expression Data Using Real-Time Quantitative PCR and the 2 ⌧⌬⌬T Method. METHODS 25, 402–408. https://doi.org/10.1006 [PubMed: 11846609]

Lyall V, Nath R, Mahmood A, 1979 Inhibition of d-glucose uptake by zinc in rat intestine. Biochem. Med 22, 192–197. 10.1016/0006-2944(79)90005-X [PubMed: 518575]

Mahler GJ, Esch MB, Glahn RP, Shuler ML, 2009a Characterization of a gastrointestinal tract microscale cell culture analog used to predict drug toxicity. Biotechnol. Bioeng 104, 193–205. 10.1002/bit.22366 [PubMed: 19418562]

Mahler GJ, Esch MB, Tako E, Southard TL, Archer SD, Glahn RP, Shuler ML, 2012 Oral exposure to polystyrene nanoparticles affects iron absorption. Nat. Nanotechnol 7, 264–271. 10.1038/nnano.2012.3 [PubMed: 22327877]

Mahler GJ, Shuler ML, Glahn RP, 2009b Characterization of Caco-2 and HT29-MTX cocultures in an in vitro digestion/cell culture model used to predict iron bioavailability. J. Nutr. Biochem 20, 494–502. 10.1016/j.jnutbio.2008.05.006 [PubMed: 18715773]

Méndez RO, Santiago A, Yepiz-Plascencia G, Peregrino-Uriarte AB, Calderón de la Barca AM, García HS, 2014 Zinc fortification decreases ZIP1 gene expression of some adolescent females with appropriate plasma zinc levels. Nutrients 6, 2229–2239. 10.3390/nu6062229 [PubMed: 24922175]

Mizumori M, Ham M, Guth PH, Engel E, Kaunitz JD, Akiba Y, 2009 Intestinal alkaline phosphatase regulates protective surface microclimate pH in rat duodenum. J. Physiol 587, 3651–3663. 10.1113/jphysiol.2009.172270 [PubMed: 19451200]

Moos PJ, Olszewski K, Honeggar M, Cassidy P, Leachman S, Woessner D, Cutler NS, Veranth JM, 2011 Responses of human cells to ZnO nanoparticles: a gene transcription study. Metallomics 3, 1199–211. 10.1039/c1mt00061f [PubMed: 21769377]

Narai A, Arai S, Shimizu M, 1997 Rapid decrease in transepithelial electrical resistance of human intestinal Caco-2 cell monolayers by cytotoxic membrane perturbents. Toxicol. Vitr 11, 347–354. 10.1016/S0887-2333(97)00026-X

Ng KW, Khoo SPK, Heng BC, Setyawati MI, Tan EC, Zhao X, Xiong S, Fang W, Leong DT, Loo JSC, 2011 The role of the tumor suppressor p53 pathway in the cellular DNA damage response to zinc oxide nanoparticles. Biomaterials 32, 8218–8225. 10.1016/j.biomaterials.2011.07.036 [PubMed: 21807406]

NIH, n.d. Zinc [WWW Document]. URL https://ods.od.nih.gov/factsheets/Zinc-HealthProfessional/

O'Halloran TV, Kebede M, Philips SJ, Attie AD, 2013 Zinc, insulin, and the liver: A a ménage à trois. J. Clin. Invest 10.1172/JCI72325

Palmiter RD, Findley SD, 1995 Cloning and functional characterization of a mammalian zinc transporter that confers resistance to zinc. EMBO J. 14, 639–649. 10.1002/j.1460-2075.1995.tb07042.x [PubMed: 7882967]

Pierce KL, James RW, 1969 US Pat. 3450656, Single Package Oleoresinous Varnish '"C"' Enamel and Process of Making Same.

Project on Emerging Nanotechnologies, 2013 Consumer Products Inventory [WWW Document]. Proj. Emerg. Nanotechnologies. URL http://www.nanotechproject.org/cpi

Ranaldi G, Marigliano I, Vespignani I, Perozzi G, Sambuy Y, 2002 The effect of chitosan and other polycations on tight junction permeability in the human intestinal Caco-2 cell line. J. Nutr. Biochem 13, 157–167. 10.1016/S0955-2863(01)00208-X [PubMed: 11893480]

Reed RB, Ladner DA, Higgins CP, Westerhoff P, Ranville JF, 2012 Solubility of nano-zinc oxide in environmentally and biologically important matrices. Environ. Toxicol. Chem 31, 93–99. 10.1002/etc.708 [PubMed: 21994124]

Renn O, Roco MC, 2006 Nanotechnology and the need for risk governance. J. Nanoparticle Res 8, 153–191. 10.1007/s11051-006-9092-7

Richter JW, Shull GM, Fountain JH, Guo Z, Musselman LP, Fiumera AC, Mahler GJ, 2018 Titanium dioxide nanoparticle exposure alters metabolic homeostasis in a cell culture model of the intestinal epithelium and *Drosophila melanogaster*. Nanotoxicology 5390, 1–17. 10.1080/17435390.2018.1457189

Robertson GL, 2012 Food Packaging: Principles and Practice, Third Edition, Handbook of Thermal Analysis and Calorimetry. 10.1016/S1573-4374(98)80007-1

Rocquet P, Auburn P, 1970 Sulphide Staining Inside Tinplate Cans and its Prevention. Br. Corros. J 5, 193–197.

Rodriguez-Yoldi MC, Mesonero JE, Rodriguez-Yoldi MJ, 1995 Study of interaction between calcium and zinc on D-galactose intestinal transport. Biol. Trace Elem. Res 50, 1–11. [PubMed: 8546879]

Roohani N, Hurrell R, Kelishadi R, Schulin R, 2013 Zinc and its importance for human health: An integrative review. J. Res. Med. Sci 18, 144–157. https://doi.org/23914218 [PubMed: 23914218]

Roselli M, Finamore A, Garaguso I, Britti MS, Mengheri E, 2003 Zinc Oxide Protects Cultured Enterocytes from the Damage Induced by Escherichia coli. J. Nutr 133, 4077–4082. [PubMed: 14652351]

Sahu D, Kannan GM, Vijayaraghavan R, 2014 Size-dependent effect of zinc oxide on toxicity and inflammatory potential of human monocytes. J. Toxicol. Environ. Heal. - Part A Curr. Issues 77, 177–191. 10.1080/15287394.2013.853224

Scott BJ, Bradwell AR, 1983 Identification of the serum binding proteins for iron, zinc, cadmium, nickel, and calcium. Clin. Chem 29, 629–633. [PubMed: 6831689]

Setyawati MI, Tay CY, Leong DT, 2015 Mechanistic Investigation of the Biological Effects of SiO_2, TiO_2, and ZnO Nanoparticles on Intestinal Cells. Small 11, 3458–3468. 10.1002/smll.201403232 [PubMed: 25902938]

Setyawati MI, Tay CY, Leong DT, 2013 Effect of zinc oxide nanomaterials-induced oxidative stress on the p53 pathway. Biomaterials 34, 10133–10142. 10.1016/j.biomaterials.2013.09.024 [PubMed: 24090840]

Song P, Onishi A, Koepsell H, Vallon V, 2016 Sodium glucose cotransporter SGLT1 as a therapeutic target in diabetes mellitus. Expert Opin. Ther. Targets 20, 1109–1125. 10.1517/14728222.2016.1168808 [PubMed: 26998950]

Song Y, Guan R, Lyu F, Kang T, Wu Y, Chen X, 2014 In vitro cytotoxicity of silver nanoparticles and zinc oxide nanoparticles to human epithelial colorectal adenocarcinoma (Caco-2) cells. Mutat. Res. - Fundam. Mol. Mech. Mutagen 769, 113–118. 10.1016/j.mrfmmm.2014.08.001

Srivastav AK, Kumar M, Ansari NG, Jain AK, Shankar J, Arjaria N, Jagdale P, Singh D, 2016 A comprehensive toxicity study of zinc oxide nanoparticles versus their bulk in Wistar rats : Toxicity study of zinc oxide nanoparticles. Hum. Exp. Toxicol 1–19. 10.1177/0960327116629530

Tahan JE, Sánchez JM, Granadillo VA, Cubillán HS, Romero RA, 1995 Concentration of Total Al, Cr, Cu, Fe, Hg, Na, Pb, and Zn in Commercial Canned Seafood Determined by Atomic Spectrometric Means after Mineralization by Microwave Heating. J. Agric. Food Chem 43, 910–915. 10.1021/jf00052a012

Tiede K, Boxall A.B. a, Tear SP, Lewis J, David H, Hassellov M, 2008 Detection and characterization of engineered nanoparticles in food and the environment. Food Addit. Contam. Part A. Chem. Anal. Control. Expo. Risk Assess 25, 795–821. 10.1080/02652030802007553

tom Dieck H, Doring F, Fuchs D, Roth H-P, Daniel H, 2005 Transcriptome and proteome analysis identifies the pathways that increase hepatic lipid accumulation in zinc-deficient rats. J. Nutr 135, 199–205. [PubMed: 15671213]

Tso C, Zhung C, Shih Y, Tseng Y-M, Wu S, Doong R, 2010 Stability of metal oxide nanoparticles in aqueous solutions. Water Sci. Technol 61, 127–133. 10.2166/wst.2010.787 [PubMed: 20057098]

Ulluwishewa D, Anderson RC, McNabb WC, Moughan PJ, Wells JM, Roy NC, 2011 Regulation of Tight Junction Permeability by Intestinal Bacteria and Dietary Components. J. Nutr 141, 769–776. 10.3945/jn.110.135657 [PubMed: 21430248]

USDA, n.d. Food Composition Databases [WWW Document]. URL https://ndb.nal.usda.gov/ndb/search/list

Vandebriel RJ, De Jong WH, 2012 A review of mammalian toxicity of ZnO nanoparticles. Nanotechnol. Sci. Appl 10.2147/NSA.S23932

Wang X, Valenzano MC, Mercado JM, Zurbach EP, Mullin JM, 2013 Zinc supplementation modifies tight junctions and alters barrier function of CACO-2 human intestinal epithelial layers. Dig. Dis. Sci 58, 77–87. 10.1007/s10620-012-2328-8 [PubMed: 22903217]

Watkins DW, Chenu C, Ripoche P, 1989 Zinc inhibition of glucose uptake in brush border membrane vesicles from pig small intestine. Pflugers Arch. 415, 165–171. 10.1007/BF00370588 [PubMed: 2594473]

Weir A, Westerhoff P, Fabricius L, Hristovski K, Von Goetz N, 2012 Titanium dioxide nanoparticles in food and personal care products. Environ. Sci. Technol 46, 2242–2250. 10.1021/es204168d [PubMed: 22260395]

Wilfinger WW, Mackey K, Chomczynski P, 1997 260/280 and 260/230 Ratios NanoDrop ® ND-1000 and ND-8000 8-Sample Spectrophotometers. BioTechniques. 22, 474–481. 10.7860/JCDR/2015/11821.5896 [PubMed: 9067025]

Wong SWY, Leung PTY, Djurišić AB, Leung KMY, 2010 Toxicities of nano zinc oxide to five marine organisms: Influences of aggregate size and ion solubility. Anal. Bioanal. Chem 396, 609–618. 10.1007/s00216-009-3249-z [PubMed: 19902187]

Yam KL, 2009 The Wiley encyclopedia of packaging technology, Wiley, A John Wiley & Sons, Inc. 10.1017/S2042169900004284

Yan H, He R, Johnson J, Law M, Saykally RJ, Yang P, 2003 Dendritic nanowire ultraviolet laser array. J. Am. Chem. Soc 10.1021/ja034327m

Zhang B, Guo Y, 2009 Supplemental zinc reduced intestinal permeability by enhancing occludin and zonula occludens protein-1 (ZO-1) expression in weaning piglets. Br. J. Nutr 102, 687 10.1017/S0007114509289033 [PubMed: 19267955]

Zijno A, De Angelis I, De Berardis B, Andreoli C, Russo MT, Pietraforte D, Scorza G, Degan P, Ponti J, Rossi F, Barone F, 2015 Different mechanisms are involved in oxidative DNA damage and genotoxicity induction by ZnO and TiO_2 nanoparticles in human colon carcinoma cells. Toxicol. Vitr 29, 1503–1512. 10.1016/j.tiv.2015.06.009

Zinc [WWW Document], n.d.

Zödl B, Zeiner M, Sargazi M, Roberts NB, Marktl W, Steffan I, Ekmekcioglu C, 2003 Toxic and biochemical effects of zinc in Caco-2 cells. J. Inorg. Biochem 97, 324–330. 10.1016/S0162-0134(03)00312-X [PubMed: 14568236]

Zoller H, Theurl I, Koch RO, McKie AT, Vogel W, Weiss G, 2003 Duodenal cytochrome b and hephaestin expression in patients with iron deficiency and hemochromatosis. Gastroenterology 125, 746–754. 10.1016/S0016-5085(03)01063-1 [PubMed: 12949720]

Highlights:

- Digested ZnO NP significantly decreased glucose transport in an in vitro model.
- Digested ZnO NP decreased the cellular surface area covered with microvilli.
- High doses of ZnO NP decreased Fe transport in a small intestine model.
- Pro-inflammatory gene IL8 was upregulated following exposure to high doses of ZnO NP.

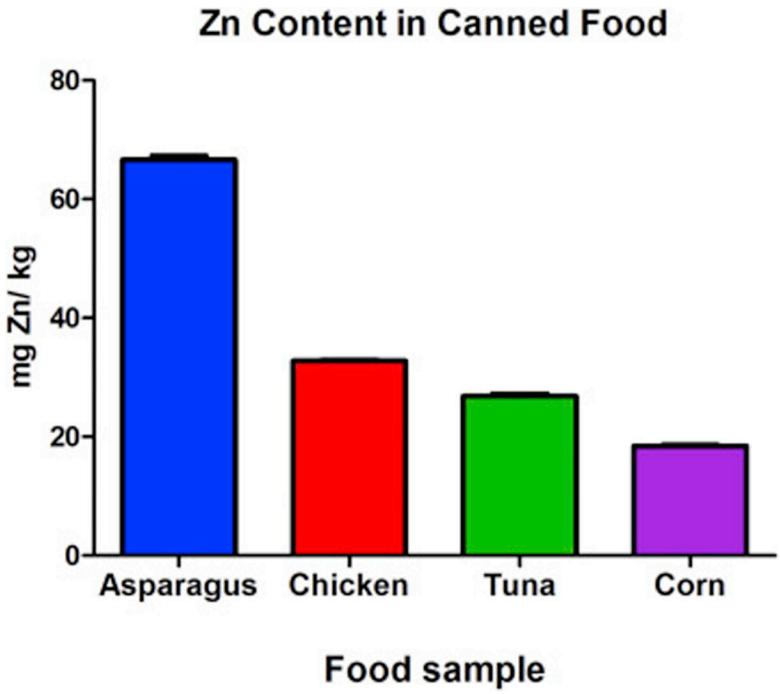

Figure 1. Zn content in canned food.

Food samples obtained from cans of food were freeze-dried and then ground to a powder. A 0.5 g aliquot of the food powder was placed into tubes and digested in HNO_3 for inductively coupled plasma mass-spectrometry (ICP-MS). Measurements were made in triplicate, mean ± SD is shown. This data was used to formulate zinc oxide nanoparticle (ZnO NP) doses for *in vitro* experiments.

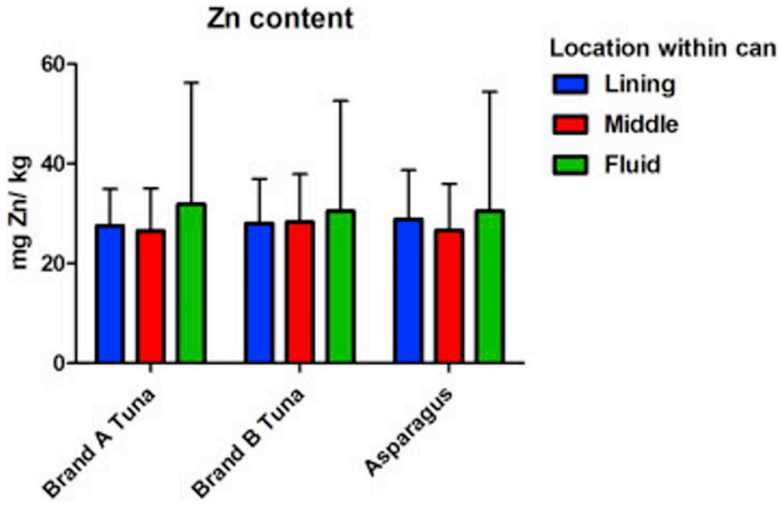

Figure 2. Zn contents based on location within the can.

Three different brands of canned food were purchased in the supermarket and the food samples were removed from three different areas of the can: touching the lining, the center, and the fluid that accumulates at the bottom. These samples were weighed before and after freeze-drying for 72 hours, and then ground into powder. A 50 mg aliquot of the powder was placed in 1.5 mL centrifuge tubes in triplicate and then digested in a heat block with 70% HNO_3 until the acid was clear with no food residue. Zn concentration was measured using inductively coupled plasma mass spectrometry (ICP-MS). Measurements were made in triplicate. Mean ± SD is shown.

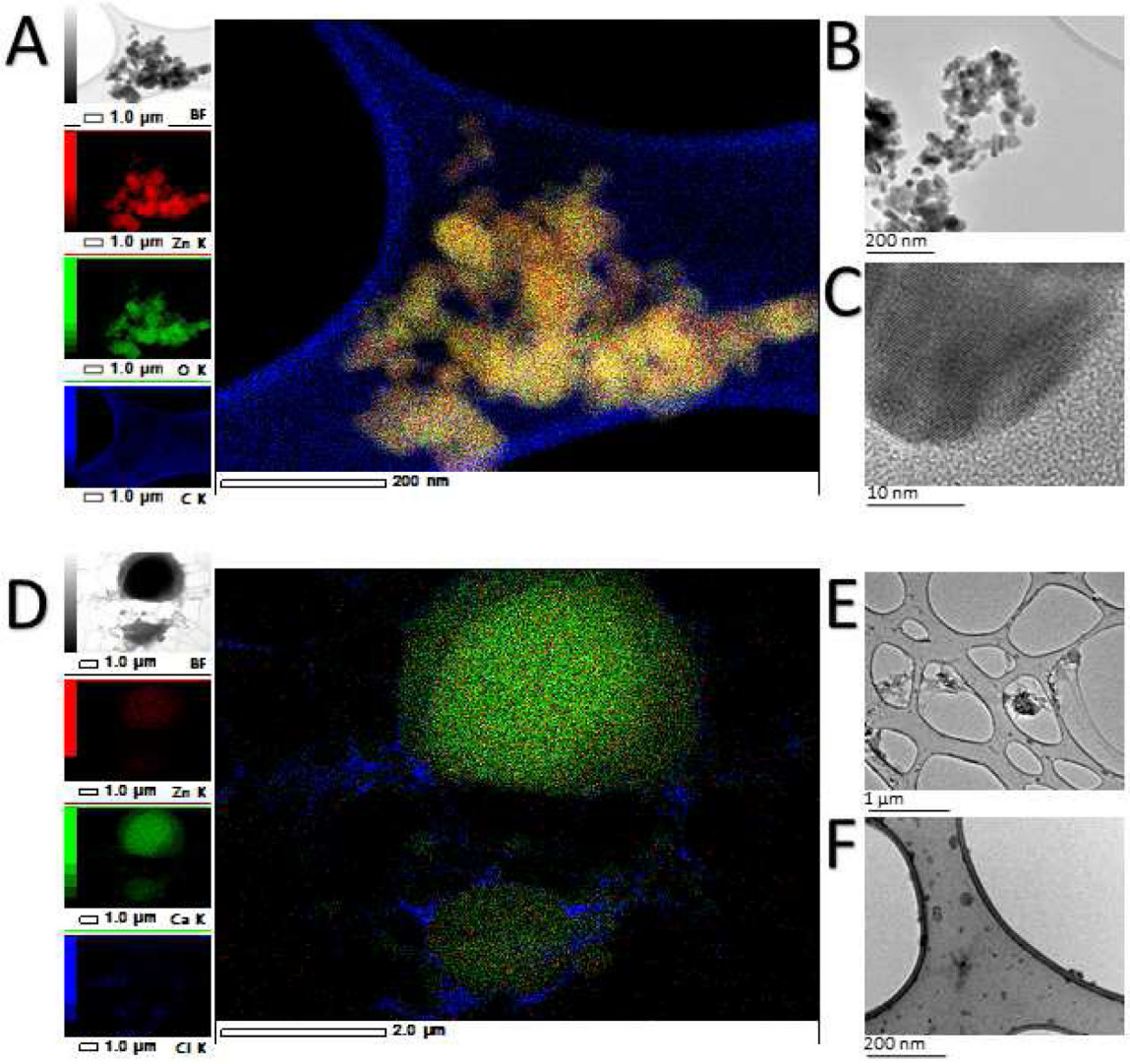

Figure 3. Nanoparticles in methanol (A-C) and following a simulated gastric and intestinal digestion (D-F).

A) Energy dispersive X-ray spectroscopy map of zinc oxide nanoparticles (ZnO NP) suspended in methanol at a concentration of 0.1mg/mL. The nanoparticles are well defined and the Zn corresponds to the size and shape of the particle in the original image. Scale bar = 200 nm. B) A ZnO NP aggregate larger than 200 nm, but the individual particles can be easily discerned. Nanoparticles ranged between 15-23 nm in size. Scale bar = 200 nm. C) A high magnification of a single ZnO NP in which the lattice fringe of the NP is visible. Scale bar = 10 nm. D) Energy dispersive X-ray map of 1×10^{11} digested ZnO nanoparticles/mL. The crystalline form of the NP has disappeared, and the Zn has accumulated in certain areas of the grid, associating mainly with Ca. This is evidence that the NP dissolve in complex solutions. Scale bar = 2 µm. E & F) Transmission Electron Microscope (TEM) views of medium digest. Scale bar = 1µm and 200 nm, respectively.

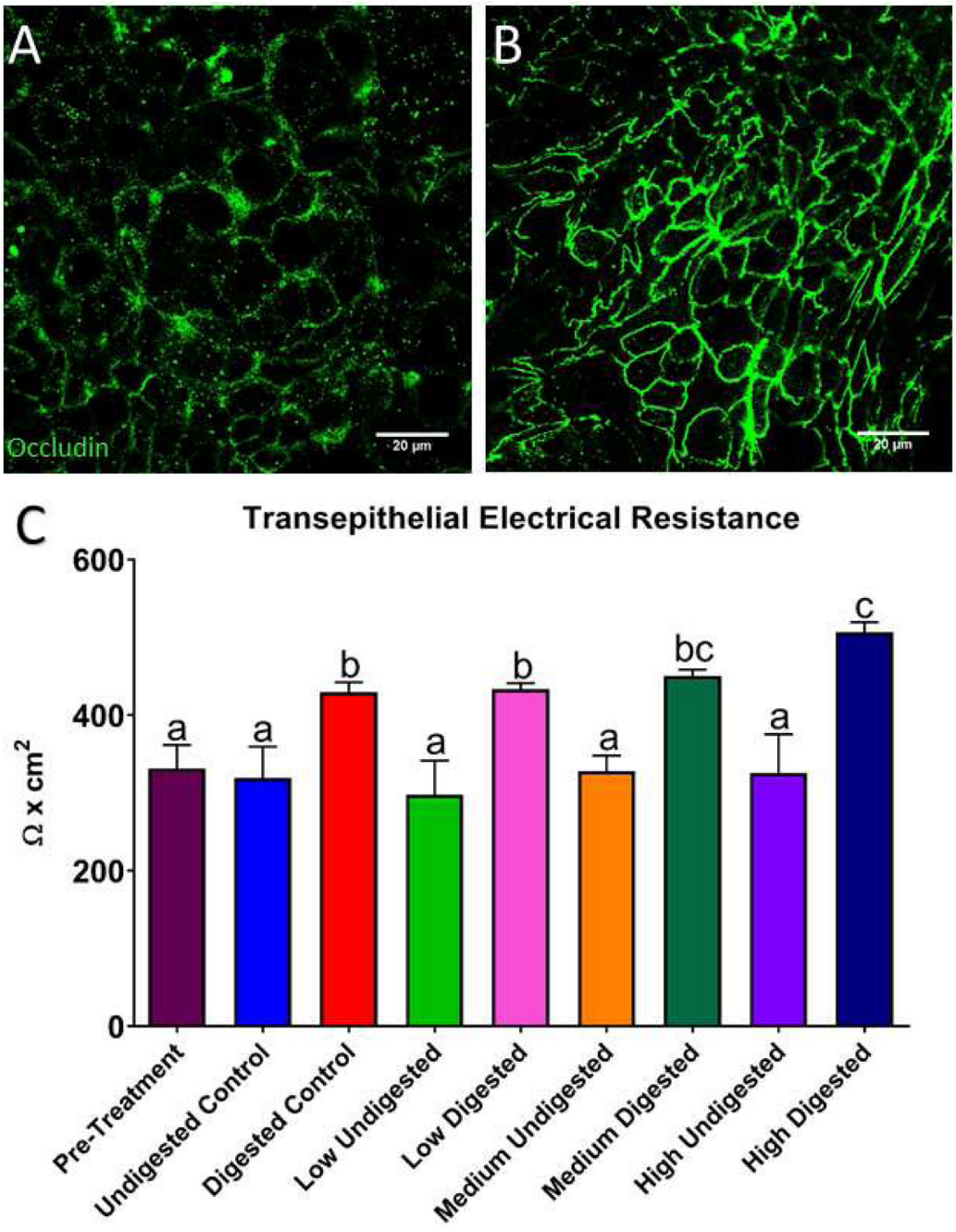

Figure 4. Occludin immunocytochemistry (ICC, A and B) and transepithelial electrical resistance (TEER, C).

A) Immunocytochemistry of Caco-2/HT29-MTX monolayers maintained in low-mineral MEM medium and supplemented with ^{58}Fe. B) ICC of control cells maintained in low-mineral MEM medium supplemented with ^{65}Zn isotope. The addition of Zn improves the definition of the tight junction protein occludin. C) Transepithelial resistance (TEER) of cells treated with 9.7×10^{-6} mg/mL undigested and digested ZnO NPs for 4 hours. Bars that do not share any letters are significantly different according to a one-way ANOVA with Tukey's post test ($p < 0.05$). Mean ± SD is shown.

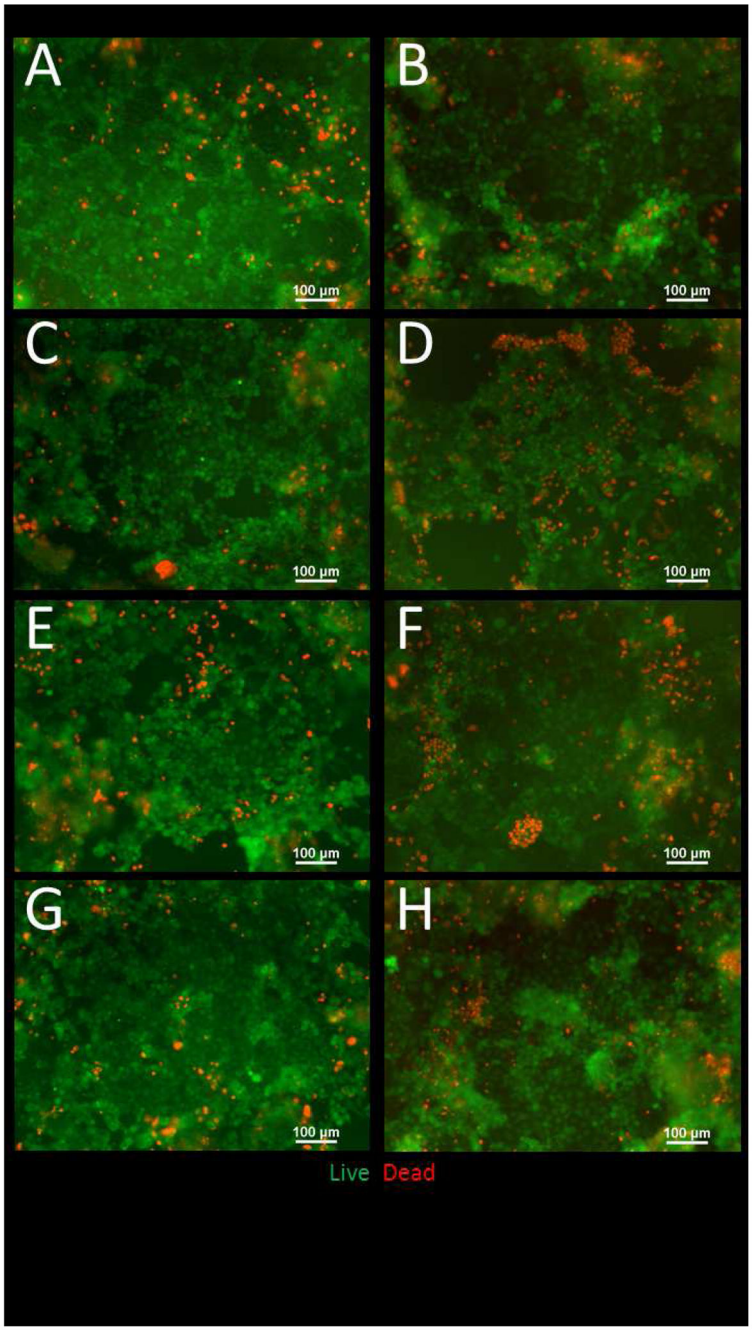

Figure 5. Cell viability after exposure to zinc oxide nanoparticles (ZnO NP).

Cells were exposed to low, medium and high doses of digested and undigested ZnO NP for 4 hours prior to the cell viability assessment. For panels A & B, data was analyzed with a one-way ANOVA with Tukey's multiple comparison test and data was considered significant at $p<0.05$. Mean±SD is shown, n = 32. In panel C a two-way ANOVA compares the means of each column to each other, Tukey groups are shown and data was considered significant at $p<0.05$. Mean±SD is shown, n = 32. In panel C, error bars are clipped at the y-axis limit. Low, medium and high refer to the dose of ZnO nanoparticles, where low = 9.7×10^{-6} mg/mL, medium = 9.7×10^{-4} mg/mL, and high = 9.7×10^{-2} mg/mL.

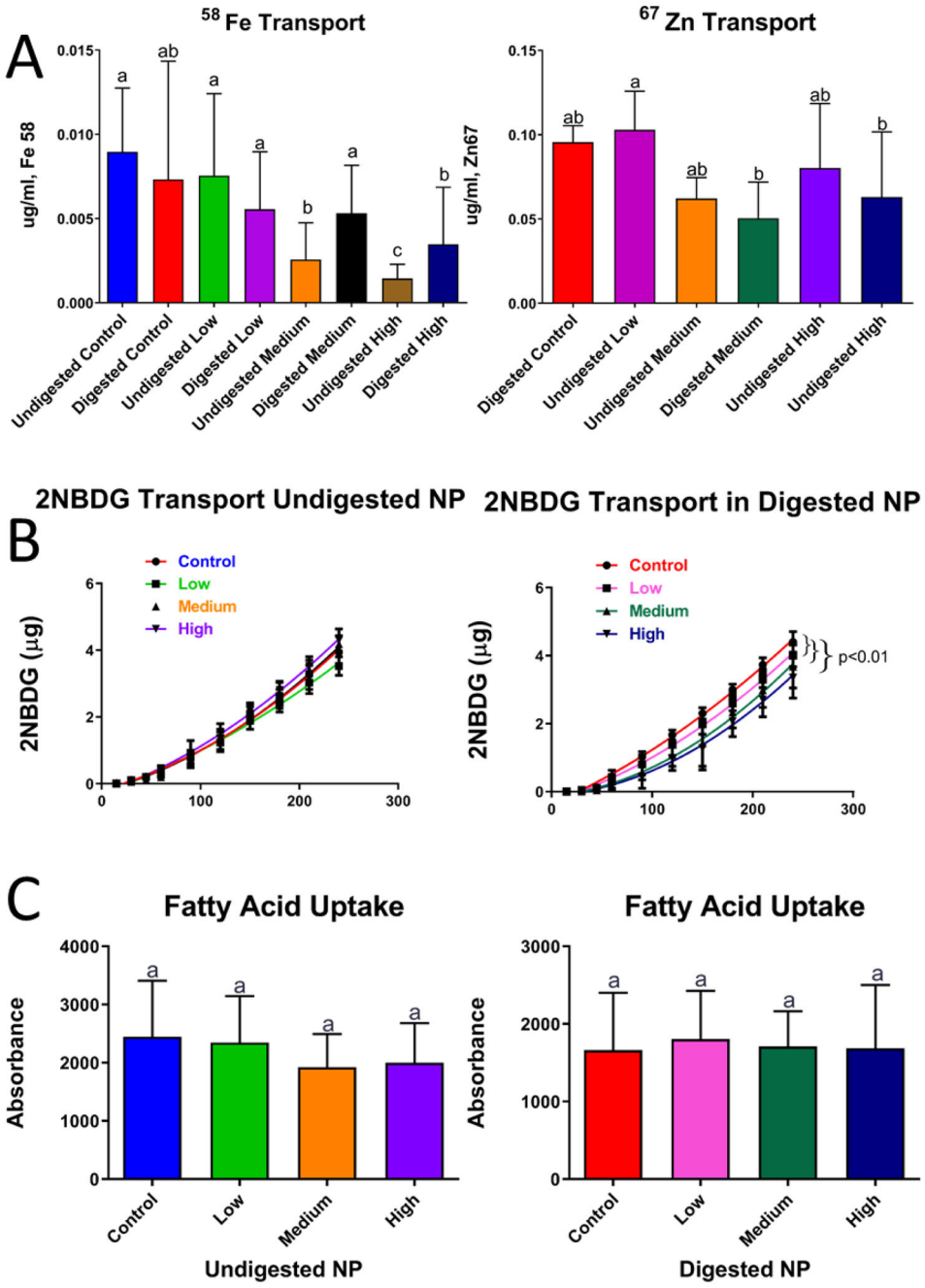

Figure 6. Live/Dead fluorescent images of Caco-2/HT29-MX co-cultures exposed to zinc oxide nanoparticles (ZnO NP).

Cells were exposed to low, medium and high doses of digested or undigested ZnO NP digests for 4 hours prior to the cell viability assessment A) Undigested Control (DMEM +10%FBS), B) digested control, C) undigested low, D) digested low, E) undigested medium, F) digested medium, G) undigested high, H) digested high. Low, medium and high refer to the dose of ZnO, nanoparticles, where low = 9.7×10^{-6} mg/mL, medium = 9.7×10^{-4} mg/mL, and high = 9.7×10^{-2} mg/mL. Digested refers to ZnO NP that were subjected to a simulated gastric and intestinal digestion.

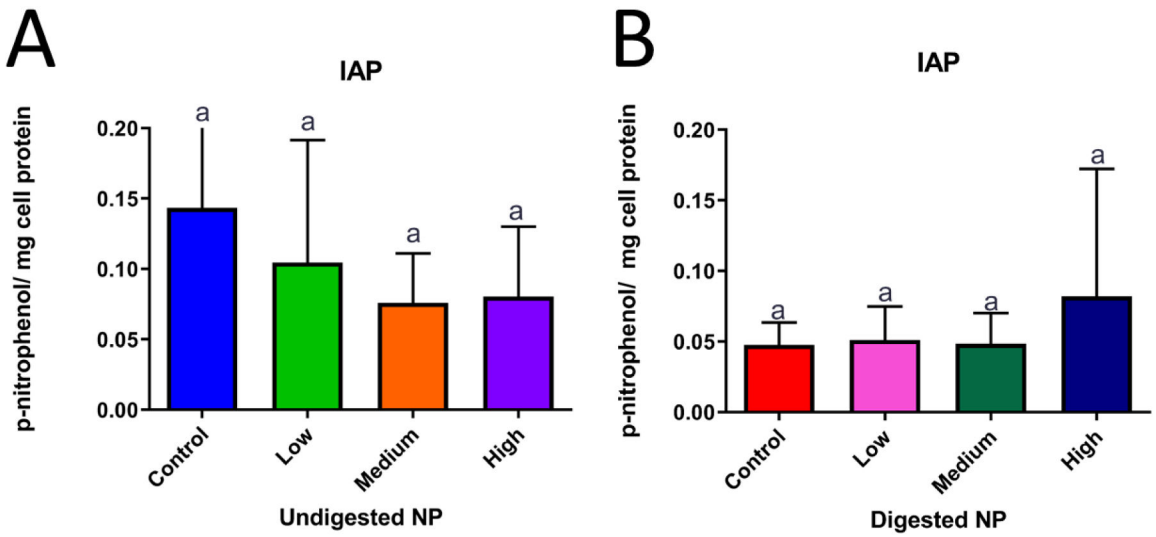

Figure 7. Overview of macronutrient transport and uptake affected by zinc oxide nanoparticles (ZnO NP).

Cells were exposed to low, medium and high doses of undigested and digested zinc oxide nanoparticles (ZnO NP) for 4 hours prior to experiments. A) Transport of ^{58}Fe stable isotope and ^{67}Zn stable isotope is representative of transport from the small intestine lumen to the bloodstream. B) Transport of glucose is representative of transport from the small intestine lumen to the bloodstream using a fluorescent glucose analog (2-NBDG) after addition of undigested and digested ZnO NP. C) Fatty acid uptake after exposure to undigested and digested ZnO. For panels A & C, data was analyzed with a one-way ANOVA with Tukey's multiple comparison test and data was considered significant at $p<0.05$. Mean±SD and Tukey groups are shown. (A,C). In panel B curve fits (solid black lines) were compared using the AICs from a quadratic model. Low, medium and high refer to the dose of ZnO nanoparticles, where low = 9.7×10^{-6} mg/mL, medium = 9.7×10^{-4} mg/mL, and high = 9.7×10^{-2} mg/mL. Digested refers to ZnO NP that were subjected to a simulated gastric and intestinal digestion.

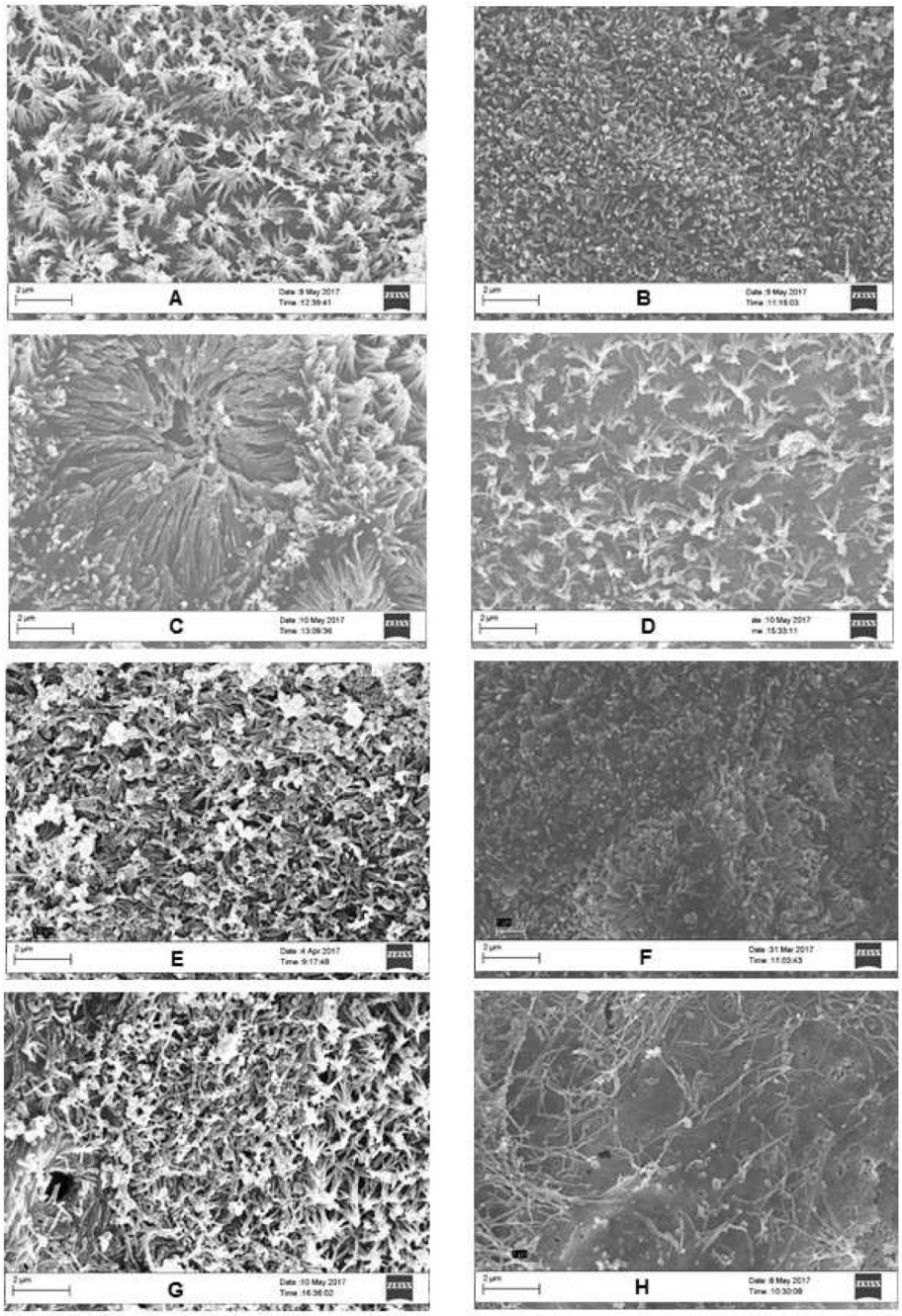

Figure 8. Intestinal Alkaline Phosphatase (IAP) Activity.

IAP activity after a 4 hour exposure to undigested and digested zinc oxide nanoparticles (ZnO NP). Bars that do not share any letters are significantly different according to a one-way ANOVA with Tukey's post test ($p < 0.05$). Mean±SD is shown, n=18. Panel A has one error bar clipped at the y-axis limit. Low, medium and high refer to the dose of ZnO NP, where low = 9.7×10^{-6} mg/mL, medium = 9.7×10^{-4} mg/mL, and high = 9.7×10^{-2} mg/mL. Digested refers to ZnO NP that were subjected to a simulated gastric and intestinal digestion.

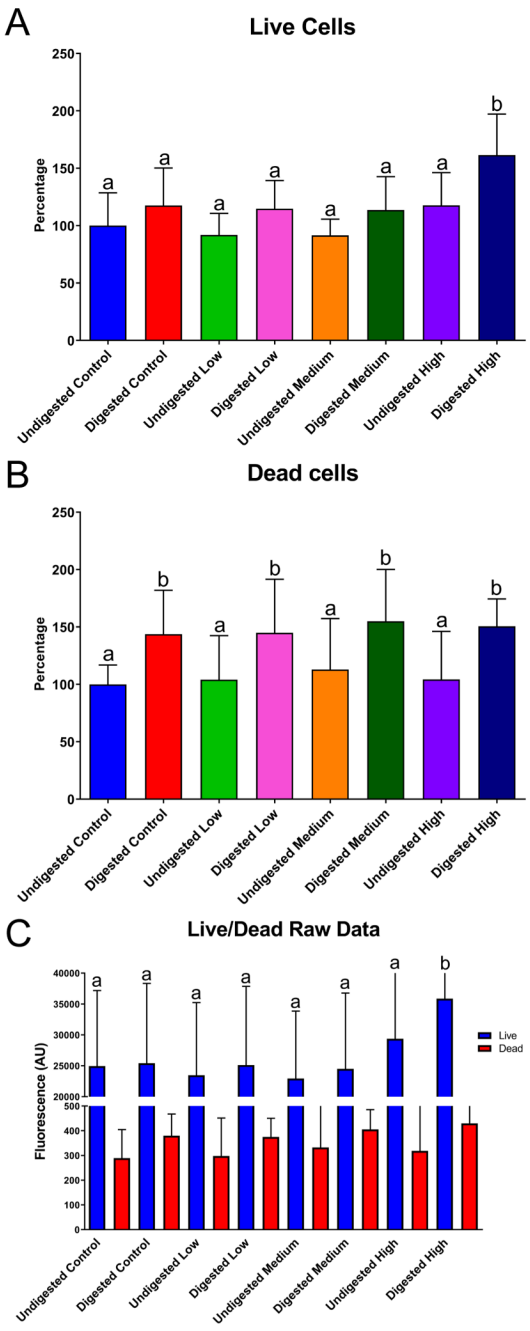

Figure 9. Scanning electron microscope (SEM) images of Caco-2/HT29-MX co-cultures exposed to zinc oxide nanoparticles (ZnO NP).

Cells were exposed to low, medium and high doses of undigested and digested ZnO NP for 4 hours prior to fixing with 4% paraformaldehyde. SEM images were taken of Caco-2/HT29-MTX co-culture microvilli. A) undigested control, B) digested control, C) undigested low, D) digested low, E) undigested medium, F) digested medium, G) undigested high, H) digested high. Low, medium and high refer to the dose of ZnO nanoparticles, where low =

9.7×10^{-6} mg/mL, medium = 9.7×10^{-4} mg/mL, and high = 9.7×10^{-2} mg/mL. Digested refers to ZnO NP that were subjected to a simulated gastric and intestinal digestion.

Table 1.

Zn content in canned foods.

Data shown are mean + SD n=3.

Sample	Average Zn Content (mg/kg)
Asparagus	66.65 ± 0.80
Chicken	32.78 ± 0.34
Tuna	26.87 ± 0.51
Corn	18.46 ± 0.30

Table 2.

Weights of food samples before and after freeze-drying.

Food	Hydrated sample weight (g)	Dehydrated sample weight (g)	Hydrated Serving weight (g)	Dehydrated serving weight (g)
Asparagus	12.4	1.2	126	12.2
Chicken	13.7	4.2	112	34.3
Tuna	12.6	5.3	112	47.1
Corn	10.3	2.0	125	24.3

Table 3.
Zinc oxide nanoparticle (ZnO NP) characterization.

Measurements performed at a ZnO NP concentration of 0.1 mg/mL in 18 MΩ deionized (DI) water and in methanol.

Instrument	Aggregate size in 18MΩ DI water	Aggregate size in methanol	Zeta potential
TEM	N/A	100-400 nm	N/A
SEM	N/A	100-400 nm	N/A
Zetasizer	130 nm	N/A	−29.9 mV
Nanosight	178 nm	N/A	N/A

Table 4.

Overview of significant changes in gene expression following exposure to zinc oxide nanoparticles (ZnO NP).

Fold increase in gene expression compared to control in response to undigested and digested ZnO NP suspensions. Stars represent treatments where significant differences were found compared to untreated

controls according to a two-way ANOVA with Tukey's post test ($p < 0.05$). Heat map is based on average values.

GENE	TREATMENT					
	Undigested			Digested		
	Low $9.7x10^{-6}$ mg/ml	Medium $9.7x10^{-4}$ mg/ml	High $9.7x10^{-2}$ mg/ml	Low $9.7x10^{-6}$ mg/ml	Medium $9.7x10^{-4}$ mg/ml	High $9.7x10^{-2}$ mg/ml
DMT1	1.46±0.13	* 1.74±0.27	*** 0.81±0.09	**** 3.69±0.41	**** 2.82±0.32	**** 3.24±0.25
DctyB	1.00±0.07	0.78±0.06	0.72±0.03	1.16±0.14	0.89±0.11	0.76±0.13
FPN1	1.25±0.08	1.38±0.19	1.35±0.17	0.90±0.07	0.98±0.16	1.69±0.18
HEPH	1.08±0.09	0.90±0.20	0.57±0.16	0.80±0.12	0.93±0.16	0.58±0.12
ZIP1	1.23±0.17	1.38±0.18	1.28±0.13	1.31±0.22	1.38±0.12	1.00±0.17
ZnT1	0.88±0.08	0.71±0.03	**** 6.32±1.08	1.03±0.09	0.89±0.15	1.08±0.10
GLUT2	** 1.85±0.44	1.31±0.27	1.07±0.08	1.16±0.26	1.23±0.14	0.94±0.19
SGLT1	1.32±0.22	0.83±0.16	0.64±0.06	0.98±0.21	0.86±0.14	0.55±0.10
FABP1	1.02±0.08	1.15±0.18	0.87±0.1	1.13±0.13	0.95±0.22	1.28±0.16
FABP2	* 1.74±0.36	1.01±0.27	0.71±0.14	0.76±0.15	0.71±0.09	0.49±0.10
TNFα	1.08±0.33	0.71±0.13	0.60±0.05	1.27±0.27	1.27±0.14	1.06±0.15
NFκB	1.23±0.18	0.83±0.17	0.69±0.06	1.22±0.22	1.29±0.14	1.05±0.18
IL8	1.52±0.3	1.19±0.20	**** 4.10±0.37	0.79±0.1	0.71±0.10	** 0.26±0.05